Journal Pre-proof

Structural optimization of natural product nordihydroguaretic acid to discover novel analogues as AcrB inhibitors

Yinhu Wang, Rawaf Alenzy, Di Song, Xingbang Liu, Yuetai Teng, Rumana Mowla, Yingang Ma, Steven W. Polyak, Henrietta Venter, Shutao Ma

PII: S0223-5234(19)31062-1

DOI: https://doi.org/10.1016/j.ejmech.2019.111910

Reference: EJMECH 111910

To appear in: *European Journal of Medicinal Chemistry*

Received Date: 13 August 2019

Revised Date: 12 November 2019

Accepted Date: 24 November 2019

Please cite this article as: Y. Wang, R. Alenzy, D. Song, X. Liu, Y. Teng, R. Mowla, Y. Ma, S.W. Polyak, H. Venter, S. Ma, Structural optimization of natural product nordihydroguaretic acid to discover novel analogues as AcrB inhibitors, *European Journal of Medicinal Chemistry* (2019), doi: https://doi.org/10.1016/j.ejmech.2019.111910.

Graphical Abstract:

Structural optimization of natural product nordihydroguaretic acid to discover novel analogues as AcrB inhibitors

Yinhu Wang [a, b, 1], Rawaf Alenzy [c, d 1], Di Song [a], Xingbang Liu [a], Yuetai Teng [a], Rumana Mowla [c], Yingang Ma [a], Steven W. Polyak [c], Henrietta Venter [c, *], Shutao Ma [a, *]

Novel nordihydroguaretic acid analogues were designed, synthesized and evaluated as AcrB inhibitors.

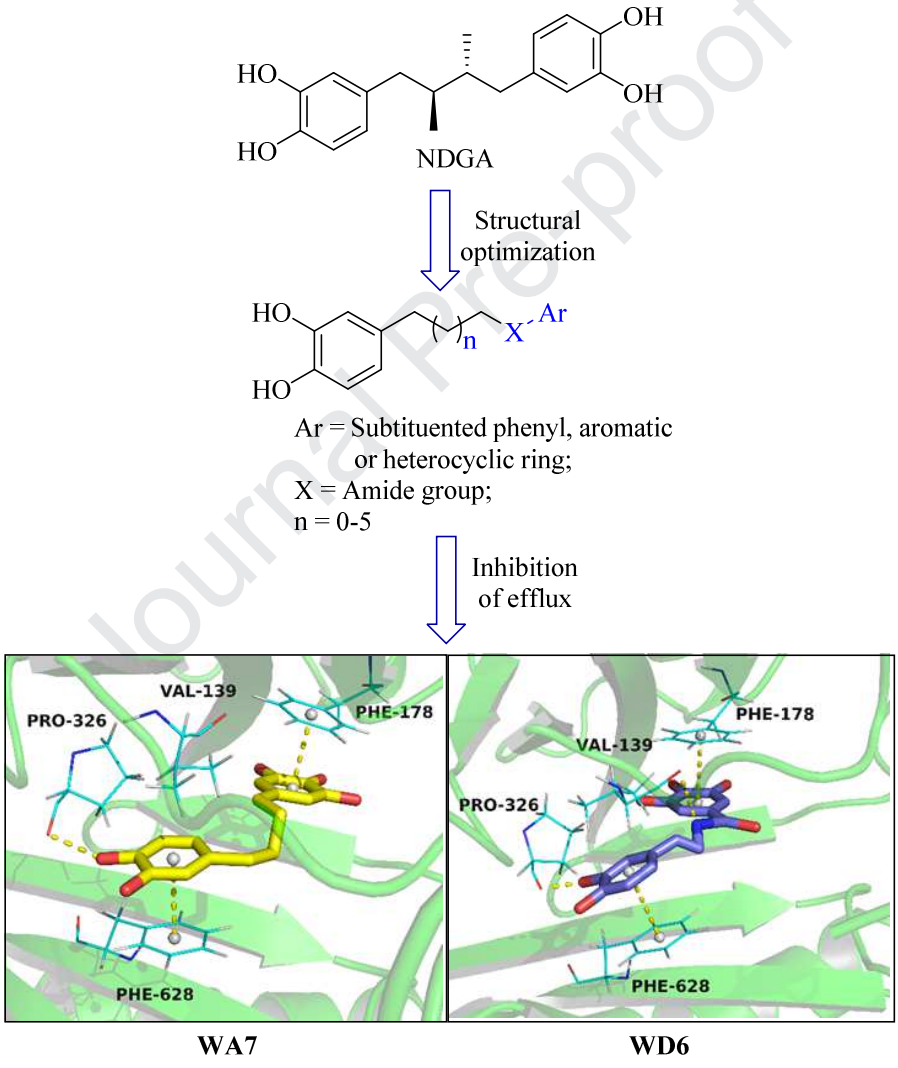

Structural optimization of natural product nordihydroguaretic acid to discover novel analogues as AcrB inhibitors

Yinhu Wang [a, b, 1], Rawaf Alenzy [c, d, 1], Di Song [a], Xingbang Liu [a], Yuetai Teng [a], Rumana Mowla [c], Yingang Ma [a], Steven W. Polyak [c], Henrietta Venter [c, *], Shutao Ma [a, *]

[a]*Department of Medicinal Chemistry, Key Laboratory of Chemical Biology (Ministry of Education), School of Pharmaceutical Sciences, Shandong University, 44 West Culture Road, Jinan 250012, China*

[b]*School of Pharmacy, Liaocheng University, Liaocheng, China*

[c]*School of Pharmacy and Medical Sciences, University of South Australia, Adelaide, SA 5000, Australia*

[d]*Department of Medical Laboratory, College of Applied Medical Sciences–Shaqra, Shaqra University, 11961, Saudi Arabia*

Running title: Nordihydroguaretic acid analogues

*Corresponding authors.

E-mail addresses: rietie.venter@unisa.edu.au (H. Venter), mashutao@sdu.edu.cn (S. Ma).

[1]These authors contributed equally

Abstract: Drug efflux pumps confer multidrug resistance to dangerous bacterial pathogens which makes these proteins promising drug targets. Herein, we present initial chemical optimization and structure-activity relationship (SAR) data around a previously described efflux pump inhibitor, nordihydroguaretic acid (NDGA). Four series of novel NDGA analogues that target *Escherichia coli* AcrB were designed, synthesized and evaluated for their ability to potentiate the activity of antibiotics, to inhibit AcrB-mediated substrate efflux and reduce off-target activity. Nine novel structures were identified that increased the efficacy of a panel of antibiotics, inhibited drug efflux and reduced permeabilization of the bacterial outer and inner membranes. Among them, **WA7**, **WB11** and **WD6** possessing broad-spectrum antimicrobial sensitization activity were identified as NDGA analogues with favorable properties as potential AcrB inhibitors, demonstrating moderate improvement in potency as compared to NDGA. In particular, **WD6** was the most broadly active analogue improving the activity of all four classes of antibacterials tested.

Keywords: Nordihydroguaretic acid; Multidrug resistance; Efflux pump; AcrB inhibitors; Structural optimization.

1. Introduction

The widespread prevalence and dissemination of multidrug-resistant (MDR) bacteria throughout the world poses a serious threat to human health. In particular, infections caused by antibiotic-resistant Gram-negative bacteria, such as *Enterobacteriaceae*, *Pseudomonas aeruginosa*, *Klebsiella pneumoniae* and *Acinetobacter baumannii*, have led to reduced or abolished efficacy of many antibacterial agents in the clinic [1-5]. Critically, only a few new classes of antibacterial drugs necessary to combat antibiotic resistance have been listed this century. In view of this situation, the World Health Organization (WHO) warns that in the near future there will be no drugs available for the treatment of serious infections caused by MDR Gram-negative bacteria unless the issue is addressed now [6-8]. Therefore, bacterial MDR has become a serious global public health concern [6, 7, 9]. Obviously, there is an urgent need to develop new solutions for the treatment of infections caused by MDR Gram-negative pathogens.

The over-expression of tripartite multidrug efflux complexes spanning the inner and outer membranes is one of major mechanisms of antibiotic resistance in Gram-negative bacteria [10-15] . Efflux pumps recognize and expel a variety of structurally diverse compounds from bacteria before they can reach their potential site of action, thereby preventing their intracellular accumulation to threshold concentrations necessary for inhibitory activity [16-21].

In MDR *Escherichia coli* and other *Enterobacteriaceae* the major drug efflux pump contributing to antibiotic resistance is AcrAB-TolC [22, 23]. This efflux pump spans both the inner and outer cell membranes as a tripartite assembly consisting of an inner membrane spanning protein (AcrB), a periplasmic adaptor protein (AcrA) and outer-membrane channel protein (TolC) [24-27]. These three separate proteins work co-operatively in a rotatory mechanism where individual subunits become alternately protonated and then engage and subsequently disengage substrate molecules [28, 29]. AcrB catalyses drug/H^+ antiport and is the protein subunit primarily responsible for substrate recognition [30-34]. AcrB can recognize an extremely broad range of substrates that are not limited to antibiotics but also includes antiseptic compounds, disinfectants, dyes, solvents, fatty acids, metal cations and virulence factors [12, 23, 35].

The inability to discover novel antibiotics to combat MDR Gram-negative bacteria prompted us to look for new strategies capable of restoring the effectiveness of existing antibiotics. Small molecule inhibitors of the AcrAB-TolC efflux pump provide an attractive route towards reversing MDR [36, 37]. Efflux pump inhibitors (EPIs) that appear in the literature have been reported to restore the activities of existing antibacterial agents by binding to AcrB, perturbing the outer membrane channel or disrupting assembly of the tripartite protein complex [19, 24, 38-42]. Despite their crucial role in MDR, there are currently no EPIs approved as antibiotic adjuvants for clinical use [43] . The recently solved crystal and cryo-electron microscopy structures of AcrB in complex with substrates or inhibitors have provided a solid basis for understanding the fundamental mechanism of drug export and rational design of high efficacy, target-specific inhibitors [28, 39, 44-46]. Crystal structures of AcrB in complex with substrates minocycline and doxorubicin [44, 47], have revealed a common substrate binding pocket that is large, flexible and rich in phenylalanine residues that allow multidrug binding via hydrophobic and π-π stacking interactions. In addition, certain polar residues also provide further opportunities to form hydrogen bonds, such as Asn274 and Gln176 [28]. Structures of inhibitor-bound AcrB have indicated that the inhibitor binding site partially overlaps with the minocycline binding site in a distal binding pocket, while another part of the inhibitor is engaged in multiple hydrophobic and π-π stacking interactions with various side chains lining an adjacent pocket known as the hydrophobic trap including Phe178, Phe610, Phe615 and Phe628 [39, 45]. EPIs binding into this site sterically hinder the functional rotation mechanism of the AcrB trimer, thereby disabling the activity of the entire efflux machinery [39, 45, 48, 49].

We recently identified nordihydroguaretic acid (NDGA, Fig. 1a) as a moderate EPI via virtual screening from a library of 50 phytochemicals [50] . In our *in silico* binding studies, it was predicted that NDGA bound into the same distal pocket described above that partially overlaps with the minocycline site (Fig. 1b). This interaction was stabilized by π-π stacking interactions between the two phenyl moieties of NDGA with aromatic side chains of Phe628, Phe178 and Phe615, and an additional hydrogen bond between a single hydroxyl group appended onto one

of the phenyl groups and the carbonyl of Pro326 and (Fig. 1c). Subsequent biological characterization revealed that NDGA acted synergistically with a broad range of antibacterials such as chloramphenicol (CAM), erythromycin (ERY) and tetraphenylphosphonium (TPP) against a MDR strain of *E. coli*. The mechanism of action of NDGA was demonstrated to be through the inhibition of AcrB using whole cell assays that measured efflux of the fluorescent Nile Red substrate. In the current study we aimed to obtain new chemotypes of NDGA with better inhibitory activity against AcrB and to gain SAR data to direct further chemical optimization. Based upon our molecular docking studies above, and our detailed knowledge of the structure of AcrB inhibitor binding site, we designed four series of novel NDGA analogues for further evaluation. In each case, the hydrogen bonding donors of the two hydroxyl groups appended onto the benzene ring on one end of the molecule were retained whilst the another end of the molecule was modified by: (1) introduction of structurally diverse groups on the benzene ring such as hydroxyl, halogen, amino, methyl and isopropyl groups to explore their interactions with the surrounding amino acid residues; (2) replacement of the benzene ring with alternative larger aromatic or heterocyclic rings such as biphenyl, naphthalene and anthracene groups, which was expected to potentiate the binding affinity for AcrB through π-π stacking or hydrophobic interactions; (3) alteration of the length of the alkyl linker to explore its accommodation within the hydrophobic binding site; (4) substitution of an amide-containing linker for the hydrophobic alkyl linker to probe additional hydrogen bonding interactions with polar amino acids lining the inhibitor binding site.

<Insert **Fig. 1**>

2. Results and discussion

2.1 Synthetic routes

The synthetic route of the NDGA analogues (**WA1**-**WA12** and **WB1**-**WB11**) is as outlined in Scheme 1. The starting material benzaldehyde was subjected to the Knoevenagel condensation with malonic acid to afford (*E*)-3-(3,4-dimethoxyphenyl)acrylic acid (**2**), which was treated with lithium aluminium tetrahydride ($LiAlH_4$) in tetrahydrofuran (THF) to give the corresponding alcohol (**3**). Then treatment of **3** with carbon tetrabromide (CBr_4) and triphenylphosphine (PPh_3) produced the brominated intermediate **4**. Subsequently, **4** was reacted with PPh_3 in refluxing toluene to give the phosphonium salts **5**. Wittig olefination of **5** with a library of appropriate aldehydes permitted the addition of a variety of phenyl and heterocyclic groups and gave the alkene intermediate **6** as a mixture of geometrical isomers. Catalytic hydrogenation of these mixtures over palladium afforded the reduction intermediate **7**, followed by subsequent demethylation with BBr_3 to generate the NDGA analogues **WA1**-**WA12** and **WB1**-**WB11**.

<Insert **Scheme 1**>

The synthetic method for 4,4'-(propane-1,3-diyl)bis(benzene-1,2-diol) (**WC1**) is shown in Scheme 2. Similarly, 3,4-dimethoxybenzaldehyde was used as starting material, which was subjected to aldol condensation with 3,4-dimethoxyacetophenone (**8**) to obtain the aldol intermediate **9**. Catalytic hydrogenation of **9** gave the reduction intermediate **10**, which was treated with sodium borohydride ($NaBH_4$) in the presence of methanol (MeOH) to provide the corresponding alcohol **11**. Then **11** was subjected to elimination to afford the alkene intermediate **12** and catalytic hydrogenation of **12** provided the intermediate **13**, which was subsequently demethylated with BBr_3 to give compound **WC1**.

<Insert **Scheme 2**>

The synthetic route for the NDGA analogue **WC2** is shown in Scheme 3. Aldol condensation of **1** with acetone afforded the ketene intermediate **14**. Catalytic hydrogenation of **14** over palladium gave the ketone intermediate **15**, which was then subjected to Wolff-Kischner reduction with hydrazine hydrate in the presence of potassium hydroxide

(KOH) to provide the intermediate **16**. Subsequently, BBr_3 demethylation of **16** gave compound **WC2**.

<Insert **Scheme 3**>

The synthetic route for the NDGA analogues **WC3** and **WC4** is shown in Scheme 4. Dicarboxylic acids (**17**) as the starting materials was subjected to chlorination with thionyl chloride ($SOCl_2$), which was followed by Friedel Crafts reaction to produce the diketone intermediate **18**. Catalytic hydrogenation of **18** over palladium gave intermediate **19**, which subsequently was demethylated with BBr_3 to yield compounds **WC3** and **WC4**.

<Insert **Scheme 4**>

The synthetic method for the NDGA analogues **WD1**-**WD10** is shown in Scheme 5. 3,4-Dimethoxybenzylamine reacted with benzoic acid with different substituents to afford the amide intermediate **21** and then demethylation of **21** produced compounds **WD1**-**WD10**. When **21** possessed nitro groups on the benzene ring, a catalytic hydrogenation reaction for **21** was first implemented, and subsequent demethylation with BBr_3 to give the corresponding NDGA analogues.

<Insert **Scheme 5**>

2.2. Antibacterial activity

The intrinsic antibacterial activity of all the NDGA analogues were initially assessed by determining the minimum inhibitory concentration (MIC) against the MDR wild type *E. coli* BW25113 expressing AcrB that is indicated as (+)AcrB and an isogenic strain with the *acrb* gene deleted that is indicated as (-)AcrB. This determined the concentration of the NDGA analogues that could be tested without producing a direct antibacterial effect in further antimicrobial synergy assays. The results showed that none of the compounds possessed intrinsic antibacterial activity against *E. coli* BW25113 at 512 µg/mL, except **WD9** with an MIC of 64 µg/mL. Likewise, none of the compounds were active against (-)AcrB cells at 64 µg/mL except **WC2** and **WD9** both of which gave an MIC value at this high concentration (data not shown). For all remaining compounds, the absence of any intrinsic antibacterial activity at 512 µg/mL allowed us to further investigate inhibition of AcrB-mediated efflux.

2.3. Ability to reverse drug resistance

The ability of the NDGA analogues to reverse antibiotic resistance conferred by the AcrAB-TolC efflux pump was next determined using a checkerboard assay [18, 43, 50]. Here, the MIC values of a panel of antibiotics were measured with *E. coli* BW25113 in the presence of varying concentrations of the tested compounds. The spectrum of EPI activity was explored using structurally unrelated antibacterials CAM, ERY, TTP and levofloxacin (LEV). Table 1 shows the data for the WA, WB and WC series that reduced the MIC values for at least one antibacterial agent by 2-fold or greater, whereas Table 2 shows the comparable data for the WD series. Ten compounds with antibacterial sensitizing activity in Table 1 were all inhibitors of TPP efflux, with **WC2** being the most potent compound that reduced the MIC value by 32-fold at 256 µg/mL. **WA5-WA7** and **WB11** were broadly active with CAM, ERY and TPP, with **WA7** and **WB11** both reducing the MIC value of TPP by 4-fold at 128 µg/mL. **WA7** also had a large effect upon CAM where it reduced the MIC value by 8-fold at the highest concentration tested. However, none of the compounds in Table 1 improved the activity of LEV.

<Insert **Table 1**>

In contrast, **WD2**, **WD6** and **WD10** in Table 2 were active when tested in combination with LEV, with **WD2** and **WD6** both reducing the MIC by 2-fold at the low concentration of 32 µg/mL. It is noteworthy that **WD6** displayed

broad activity against the four antibacterials and lowered the MIC values by 4-fold for CAM, ERY and TPP at 128 µg/mL, and the MIC value by 2-fold for LEV at 32 µg/mL. Similarly, **WD2**, **WD5**, **WD7** and **WD8** also possessed broad spectrum activity reducing the MIC values of three out of the four antibacterials in the screening panel. **WD5** and **WD9** reduced the MIC value of ERY by 4-fold at 32 µg/mL whereas **WD7** decreased the MIC values of both CAM and ERY by 4-fold at 128 µg/mL. Rifampicin (RIF) that is not a substrate of AcrB was used as a negative control. None of the compounds altered the MIC value of RIF (16 µg/mL) consistent with these compounds likely function through the AcrB efflux pump and not through alternative mechanism (s) of action [43, 51]. The findings above suggest that the compounds exert their synergistic activity through the inhibition of AcrB.

<Insert **Table 2**>

2.4. The effect of the compounds on substrate transport

The NDGA analogues that showed bioactivity in the checkerboard assays described above were characterized further to determine if they inhibited AcrB using whole cell efflux assays [43, 51]. The AcrAB-TolC substrate Nile Red was employed as this probe, which is weakly fluorescent in aqueous solutions but undergoes a significant increase in fluorescence quantum yield in non-polar environments, such as the cell membrane [52]. *E. coli* BW25113 were de-energized by treatment with the ionophore carbonyl cyanide 3-chlorophenylhydrazone (CCCP), which was followed by being preloaded with Nile Red in the absence or presence of the NDGA analogues. Following the addition of glucose to re-energize the cells, the efflux of Nile Red was measured by fluorometry. The *E. coli* strain with (-)AcrB was used as a positive control, indicating the maximum levels of Nile Red accumulation possible in the absence of efflux. The parent compound NDGA was potent in the assay, with inhibitory activity observed at the concentration of 50-100 µM (Fig. 2). In remarkable contrast, **WA5**, **WA7**, **WC1** and **WD6-WD8** were weakly active, with inhibitory activity only observed at the highest concentration tested (500 µM). The moderate activity was observed for **WC2**, **WC4**, **WD4** and **WD5** at the concentration of 100-200 µM. The most potent inhibitory activity was measured for **WA9**, **WA10**, **WB11**, **WC3** and **WD9** at the concentration of 50-100 µM (Fig. 2), which could completely inhibit efflux to the level of the pump-deleted strain, similar to NDGA.

<Insert **Fig. 2**>

2.5. The effect of the compounds on the bacterial outer membrane

Compounds that permeabilize either the inner or outer bacterial membranes may show synergistic activity with antibiotics in a mechanism independent of AcrAB-TolC [53]. To determine if the potentiation of the antibiotic activity observed above could be due to permeabilization of the outer membrane, the rate of hydrolysis of a chromogenic β-lactam, nitrocefin was assayed using intact *E. coli* BW25513 [54] . Hydrolysis of nitrocefin by the bacterial β-lactamase produces a colored product that can be measured spectrometrically at 490 nm. The rate of nitrocefin hydrolysis is limited by the rate of diffusion across the outer membrane, but this may be accelerated due to outer membrane permeabilization [51]. Polymyxin B (PMB) was used as a positive control as this agent is known to damage the bacterial outer membrane (red line, Fig. 3). Disruption of the outer membrane was observed when cells were treated with 256 µg/ml NDGA with increased absorbance measured over the time course that was above the untreated control (blue lines, Fig. 3). Similar off-target activity was observed for **WA9** and **WA10**. **WC3** was particularly toxic as the yield of product formed approached that measured for polymyxin B, so this compound was discarded from further evaluation. The NDGA analogues with desirable low permeabilization activity included **WA5**, **WA7**, **WB11**, **WC1-WC4**, **WD2** and **WD4-WD9**. For these agents, we could conclude that their synergism with known antibacterials was not due to the secondary mechanism of membrane permeabilization.

<Insert **Fig. 3**>

2.6. The effect of the compounds on the bacterial inner membrane

Finally, off-target activity caused by chemical damage to the inner membrane was addressed. As AcrAB-TolC is powered by the proton motive force across the bacterial inner membrane, compounds that perturb the proton gradient could also indirectly inhibit efflux [4, 11, 51]. The ability of NDGA analogues to cause depolarization of bacterial transmembrane potential (Δψ) was evaluated by using the fluorescent membrane potential-sensitive probe 3,3-diethyloxacarbocyanine iodide ($DiOC_2(3)$). Bacteria were first energized by the addition of glucose to establish the proton motive force (negative and basic inside the cell), then treated with $DiOC_2(3)$ and increased fluorescence measured due to the aggregation of the positively charged probe as it entered cells through passive diffusion. Upon addition of the ionophore CCCP, the Δψ was dissipated and the fluorescence intensity reduced to the level before glucose stimulation (See Fig. 4, blue curves representing bacteria not challenged with compound) [18, 43, 55]. Those compounds that disrupted the inner membrane consequently disturbed the proton gradient resulting in no accumulation of fluorescence signal. Severe membrane disruption activity was observed with the parent compound NDGA at concentrations of 64 µg/mL or greater (Fig. 4). This unwanted off-target activity was not investigated in the initial report. Similar low toxicity was observed at 128 µg/mL for **WA5** and **WC2**. However, the off-target activity was reduced for **WA7** (128 g/mL), **WB11** (16 µg/mL) and **WC4** (64 µg/mL). Likewise, **WD4-WD8** also displayed favorable properties with neither **WD4-WD6** showing toxicity at 64 µg/mL. It was noteworthy that **WD7** and **WD8** was still inactive in the assay at 128 µg/mL. Unexpectedly, poor accumulation of $DiOC_2(3)$ was observed when bacterial were treated with **WD9**, consistent with damage to the inner membrane. Consequently, **WA7**, **WB11**, **WC2**, **WC4** and **WD4-WD8** with a mechanism of action consistent with the inhibition of AcrB were confirmed.

<Insert **Fig. 4**>

2.7. Molecular docking

To aid in the interpretation of the biological findings and the establish SAR data to guide future chemical optimization, molecular modelling studies were performed. Crystal structures of AcrB in complex with substrates and inhibitors have revealed that the binding pocket of AcrB is rich in phenylalanine residues Phe136, Phe178, Phe610, Phe615, Phe628 that stabilize ligand binding through hydrophobic and π-π stacking interactions. In addition, certain polar amino acid residues provide hydrogen bonding potential such as Asn274, Gln176 and Pro326 [4, 28, 47]. Building upon our earlier in silico binding studies with NDGA (Fig. 1), we designed the NDGA analogues that retained the hydrogen bond donor nature of phenolic hydroxyl groups at the one end of the molecule. Pharmacomodulations then involved the introduction of the structurally diverse groups into the benzene ring at the other end of the molecule (**WA1**-**WA12**) to explore their interactions with the surrounding polar and non-polar amino acid residues in the binding pocket of AcrB. Further, we replaced the benzene ring with aromatic or heterocyclic rings owning a larger spatial structure (**WB1**-**WB11**) to explore their binding affinity for AcrB via π-π stacking or hydrophobic interactions. In addition, we changed the length of the alkyl linker between the two benzene rings (**WC1**-**WC4**) to explore their adaptability in the hydrophobic cavity of the binding pocket. Finally, we substituted the alkyl linker in NDGA using an amide-containing linker (**WD1**-**WD10**) to probe additional hydrogen bonding interaction with the amino acid residues.

After the exhaustive biological characterization of the test compounds, eight NDGA analogues specifically acting on AcrB were identified as AcrB inhibitors in this study, namely **WA7**, **WB11**, **WC2**, **WC4** and **WD4-WD8**. In order to reasonably explain the above biological data and visually discuss the binding mode of the bioactive compounds with AcrB, we selected **WA7** and **WD6** as representative compounds for molecular docking. Molecular docking software SYBYL-X2.0 was used to predict the mode of binding in AcrB (PDB: 5ENO), and the docking results visualized by PYMOL, as shown in Fig. 5. The docking results indicated that the binding modes of **WA7** and **WD6** were similar to that of the parent compound NDGA. The phenolic hydroxyl groups at the one end of the molecule

bond to oxygen of Pro326 by hydrogen bond interaction, while two benzene rings at both ends of the molecule were stabilized by interactions with the amino acids Phe628 and Phe178 via π-π stacking interactions. Moreover, the oxygen atom of the amide group on the linker of **WD6** formed an additional hydrogen bond with the Val139, which may be the reason why the bioactivity of WD series was generally better than that of the other series. The additional binding interactions likely improve on-target recognition of AcrB that help minimize the off-target activities observed with NDGA.

<Insert **Fig. 5**>

On the whole, four series of novel NDGA analogues were designed, synthesized and characterized for their ability to inhibit the AcrAB-TolC efflux pump in *E. coli*. The preliminary SARs derived from this study indicate that: (1) the sensitizing activity of the NDGA analogues is closely related to the substituents on the benzene ring in their molecules, and hydrophilic groups are preferred; (2) the replacement of the benzene ring with aromatic or heterocyclic rings possessing a large steric effect is unfavorable for retaining potency; (3) the intermediate linker is best with a four-atom chain, and the introduction of the amide-containing linker can improve the efficacy. Furthermore, NDGA was observed to possess significant and undesirable activity such as off-target effect in the assays of measuring the permeabilization of the bacterial inner and outer membranes. Through the structural optimization of NDGA, new chemical structural types specifically targeting AcrB were identified, which displayed superior or comparable efficacy to NDGA, indicating a successful chemical modification in this program. More importantly, the above SARs provide some valuable information in guiding the further structural optimization of NDGA as well.

Noteworthy are the WD series possessing the amide-containing linker that generally exhibit better efficacy against the AcrB-expressing strain than that of the WA, WB and WC series, which is probably due to an additional hydrogen bond of the oxygen atom of the amide group with the Val139 in the pocket, thereby improving binding affinity for AcrB. Among the best compounds, **WD6** showed the best efficacy and decreased the MIC values by 4-fold for CAM, ERY and TPP, and the MIC value by 2-fold for LEV at a lower concentration than that of its parent NDGA. **WD5** and **WD9** lowered the MIC value of ERY by 4-fold at 32 μg/mL, whereas **WD7** and **WD8** at 128 μg/mL reduced the MIC values of both CAM and ERY by 4-fold and by 2-fold, respectively. In contrast, the WA, WB and WC series all possess a hydrophobic alkyl linker in their structure. In the WA series, **WA5**-**WA7** were broadly active with CAM, ERY and TPP, and particularly **WA7** reduced not only the MIC value of CAM by 8-fold at 256 μg/mL, but also the MIC value of TPP by 4-fold at 128 μg/mL. In the WB series, only **WB11** containing pyrene group showed broadly synergism with CAM, ERY and TPP, reducing the MIC value of TPP by 4-fold at 128 μg/mL. This could be because the pyrene moiety could block the freedom of mutual rotation of the ring in the structure and might facilitate a good fit within the AcrB binding pocket. However, none of the compounds in the WA, WB and WC series improved the activity of LEV. Moreover, the optimal length of the alkyl linker that connects two aromatic rings was four atoms, which could ensure that the two aromatic rings simultaneously interacted with the corresponding amino acid residues (Phe178 and Phe628) via π-π stacking or hydrophobic interactions, thereby potentiating the binding affinity for AcrB. Subsequently, in order to further confirm the efflux inhibition activity and specificity of AcrB, the active compounds were selected to determine their efflux inhibition ability of Nile Red, and the effect on outer and inner membrane permeabilization. Consequently, **WA7**, **WB11**, **WC2**, **WC4** and **WD4**-**WD8** were found to exhibit the following characteristics of an ideal AcrB inhibitor, as described by Lomovskaya et al. [11, 51]: (1) it potentiated the activity of various antibacterial agents that are substrates of AcrAB-TolC; (2) it did not reduce the MIC values of the agents that were not its substrates (e.g., RIF); (3) it had no effect on susceptible strains ((-)AcrB); (4) it decreased the level of extrusion of AcrB substrates (e.g., Nile Red); (4) it did not permeabilize the outer membrane; (5) it did not disturb the proton gradient of AcrB across the inner membrane.

3. Conclusions

In this study, thirty-seven compounds were designed, synthesized and evaluated for their AcrB inhibition activity. The results revealed that nine compounds (**WA7**, **WB11**, **WC2**, **WC4** and **WD4-WD8**) identified as ideal AcrB inhibitors were able to reduce the MIC value of at least one antibiotic tested by 2- to 32-fold. They also inhibited Nile red efflux at reasonable concentration and acted specifically on the AcrB efflux pump. Among the above compounds with characteristics of ideal AcrB inhibitors, the best candidates **WD6**, **WA7** and **WB11** have broad-spectrum antimicrobial sensitization activity. In particular, **WD6** is the most active analogue improving the activity of all four classes of antibacterials tested. Although this study obtained a promising group of potential AcrB inhibitors, the most active compounds displayed only moderate sensitizing properties. Therefore, further optimization of NDGA analogues with potent AcrB-targeted antibacterial activity should continue to be investigated.

4. Experimental

4.1. Chemistry

All reagents and chemicals that are of analytical grade in the present study were commercially available and used without further purification. Analytical thin-layer chromatography (TLC) was performed using silica gel GF254 plates to monitor the reaction progress. Flash column chromatography were carried out using silica gel 60 (particle size 0.040-0.063 mm) for separation and purification of crude products. ^{1}H NMR and ^{13}C NMR spectra were recorded on Bruker instrument at 400 or 600 MHz, and chemical shifts (δ) are reported in parts per million (ppm). Electron-spray ionization mass spectra in positive mode (ESI-MS) data were registered on API 4000 instrument (Applied Biosystems, Connecticut, USA). Analytical high-performance liquid chromatography (HPLC) was carried out on an Agilent 1200 Series equipment coupled to ultraviolet-visible detector (UVD) at 230 nm with a Diamonil C18 reversed phase column (150 × 4.6 mm, 5 μm), eluted by water and acetonitrile. The effective chromatogram was obtained using the mobile phase of acetonitrile: water (60:40, vol./vol.) with a flow rate of 1.0 mL/min. The purity of the tested compounds as determined by analytical HPLC was more than 95%.

*4.1.1. (E)-3-(3,4-Dimethoxyphenyl)acrylic acid (**2**)*

A mixture of 3,4-dimethoxybenzaldehyde (**1**) (9.50 g, 57.20 mmol), malonic acid (23.80 g, 228.80 mmol) and piperidine (1 mL) in pyridine (60 mL) was heated at 70 °C for about 6 h. Upon completion, pyridine was removed in vacuo. The residue obtained was dissolved in 15 % solution of NaOH (100 mL), stirred at room temperature for 0.5 h, and extracted with ethyl acetate (EtOAc) (60 mL). The water phase was acidified with concentrated HCl to a pH value of less than 2. The resulting precipitate was filtered off, washed with water, and dried in vacuo to give (*E*)-3-(3,4-dimethoxyphenyl)acrylic acid (**2**) (10.70 g, 90%). mp:181–183 °C.

*4.1.2. 3-(3,4-Dimethoxyphenyl)propan-1-ol (**3**)*

To a stirred suspension of $LiAlH_4$ (2.73 g, 71.94 mmol) in anhydrous THF (50 mL) was added **2** (10.00 g, 48.03 mmol) as a solid in portions over 30 min. After addition, the resulting reaction mixture was refluxed for 5 h, cooled to room temperature, and quenched with MeOH (20 mL). The resulting suspension was filtered under vacuum, washed in turn with EtOAc (100 mL) and brine, and dried over anhydrous Na_2SO_4. The organic extracts were concentrated in vacuo to yield a pale yellow oil (**3**, 7.80 g, 83%). ^{1}H NMR (400 MHz, $CDCl_3$) δ 6.79 (d, *J* = 8.1 Hz, 1H, H-5), 6.74 (d, *J* = 6.1 Hz, 2H, H-2 and H-6), 3.86 (s, *J* = 5.7 Hz, 6H, 2×OCH_3), 3.67 (t, *J* = 6.2 Hz, 2H, $\underline{CH_2}OH$), 2.66 (t, *J* = 7.6 Hz, 2H, Ph-CH_2), 1.88 (q, *J* = 7.3 Hz, 2H, $\underline{CH_2}CH_2OH$), 1.74 (s, 1H, $CH_2CH_2\underline{OH}$).

*4.1.3. 4-(3-Bromopropyl)-1,2-dimethoxybenzene (**4**)*

After **3** (7.60 g, 38.73 mmol) was dissolved in dichloromethane (DCM) (50 mL), along with CBr_4 (13.50 g, 40.67 mmol), the reaction mixture was cooled to 0 °C, and PPh_3 (10.68 g, 40.67 mmol) was added slowly. The resultant reaction solution was stirred for 2 h, and the reaction solvents were removed under reduced pressure. The residue was purified by flash column chromatography (petroleum ether/EtOAc) to produce a colorless oil (**4**, 8.72 g, 87%).

*4.1.4. (3-(3,4-Dimethoxyphenyl)propyl)triphenylphosphonium bromide (**5**)*

To a solution of **4** (7.00 g, 27.01 mmol) in toluene (80 mL) were added PPh_3 (21.25 g, 81.03 mmol) under an atmosphere of nitrogen. The resulting reaction mixture was heated to reflux for 36 h. After cooling to room temperature, the deposits were filtered, washed with toluene, and dried in vacuo to give the phosphonium salts **5** (8.70 g, 62%). mp: 169–171°C; ^{1}H NMR (400 MHz, $CDCl_3$) δ 8.04–7.41 (m, 15H, Ph-H), 6.90–6.65 (m, 3H, H-2、H-5 and H-6), 3.85 (d, *J* = 2.8 Hz, 6H, 2×OCH_3), 2.99 (t, *J* = 7.0 Hz, 2H, Ph-CH_2), 1.93 (t, *J* = 12.3 Hz, 2H, $\underline{CH_2}PPh_3$), 1.71 (q, 2H, $CH_2\underline{CH_2}CH_2$).

*4.1.5. General procedure for the preparation of compounds (**6**)*

The phosphonium salts **5** (1.53 mmol) was dissolved in in dry THF (12 mL) at 0 °C, and to this solution were added slowly n-butyllithium (1.84 mmol) and corresponding aromatic aldehyde (1.84 mmol). The reaction mixture was then stirred for 5 h at room temperature. Upon completion of the reaction, the mixture was quenched with water (30 mL), extracted with EtOAc (3 × 25 mL), washed with brine, and over anhydrous Na_2SO_4. The organic extracts were concentrated in vacuo to give a residue, which was purified by flash column chromatography (petroleum ether/EtOAc) to afford an alkene products **6** in the yields of 45-82%.

*4.1.6. General procedure for the preparation of compounds (**7**)*

Palladium on charcoal (10%, 50 mg) was added to a stirring solution of **6** (0.83 mmol) in MeOH–EtOAc (4:1) (10 mL) and the reaction mixture was stirred under a hydrogen balloon at room temperature for 24 h. The reaction mixture was filtered and the residue washed with EtOAc (2 × 15 mL). The combined organic layers were concentrated under reduced pressure to give a crude product (**7**), which was used directly for the next step without further purification.

*4.1.7. General procedure for the preparation of **WA1**-**WA12** and **WB1**-**WB11***

To a solution of **7** (0.38 mmol) in DCM (8 mL) at -78 °C was added BBr_3 (1.52 mmol) slowly. The resulting solution was allowed to warm to room temperature and stirred for 1 h, which was then poured into iced water (40 mL). The resultant mixture was extracted with DCM (3 × 20 mL), dried over anhydrous Na_2SO_4, and filtered. The filtrate was concentrated in vacuo and the residue was purified by flash column chromatography (DCM/MeOH) to produce the crude products, which were crystallized from ether-hexane to afford the target compounds **WA1**-**WA12** and **WB1**-**WB11**.

*4.1.7.1. 4-(4-Phenylbutyl)benzene-1,2-diol (**WA1**).* White solid, yield 56%, mp 71–73 °C, R_f = 0.65 (DCM/MeOH = 10:1); ^{1}H NMR (400 MHz, DMSO-d_6) δ 8.68 (s, 1H, OH), 8.58 (s, 1H, OH), 7.29–7.22 (m, 2H, H-2′ and H-6′), 7.19–7.12 (m, 3H, H-3′, H-4' and H-5′), 6.60 (d, *J* = 8.0 Hz, 1H, H-5), 6.53 (d, *J* = 2.0 Hz, 1H, H-2), 6.39 (dd, *J* = 8.0, 2.1 Hz, 1H, H-6), 2.57 (t, *J* = 7.2 Hz, 2H, Ph′-CH_2), 2.41 (t, *J* = 7.1 Hz, 2H, Ph-CH_2), 1.58–1.46 (m, 4H, $CH_2\underline{CH_2}\underline{CH_2}CH_2$); ^{13}C NMR (150 MHz, $CDCl_3$) δ 143.28, 142.60, 141.21, 135.94, 128.44 (2C), 128.27 (2C), 125.66, 120.89, 115.52, 115.27, 35.82, 35.07, 31.14, 30.99; ESI-MS *m/z* calcd for $C_{18}H_{18}O_4F_3$ [M + CF_3COO]$^-$ 355.1, found 355.4.

*4.1.7.2. 4-(4-(p-Tolyl)butyl)benzene-1,2-diol (**WA2**).* White solid, yield 37%, mp 70–72 °C, R_f = 0.68 (DCM/MeOH = 10:1); ^{1}H NMR (600 MHz, DMSO-d_6) δ 8.68 (s, 1H, OH), 8.57 (s, 1H, OH), 7.09–7.01 (m, 4H, H-2′, H-3′, H-5′ and H-6′), 6.59 (d, *J* = 7.9 Hz, 1H, H-5), 6.52 (d, *J* = 2.1 Hz, 1H, H-2), 6.39 (dd, *J* = 8.0, 2.1 Hz, 1H, H-6), 2.53 (d, *J* = 7.2 Hz, 2H, Ph-CH_2), 2.40 (t, *J* = 7.3 Hz, 2H, Ph′-CH_2), 2.25 (s, 3H, CH_3), 1.50 (dddd, *J* = 23.5, 12.1, 9.0, 5.0 Hz, 4H, $CH_2\underline{CH_2}\underline{CH_2}CH_2$); ^{13}C NMR (150 MHz, $CDCl_3$) δ 143.29, 141.22, 139.51, 135.95, 135.06, 128.95 (2C), 128.30 (2C), 120.85, 115.50, 115.23, 35.36, 35.09, 31.16, 31.13, 21.00; ESI-MS *m/z* calcd for $C_{19}H_{20}O_4F_3$ [M + CF_3COO]$^-$ 369.1, found 369.2.

*4.1.7.3. 4-(4-(4-Isopropylphenyl)butyl)benzene-1,2-diol (**WA3**).* White solid, yield 48%, mp 72–74 °C, R_f = 0.24 (DCM/MeOH = 30:1); ^{1}H NMR (400 MHz, DMSO-d_6) δ 8.68 (s, 1H, OH), 8.59 (s, 1H, OH), 7.12 (d, *J* = 8.1 Hz, 2H, H-3′ and H-5′), 7.07 (d, *J* = 8.0 Hz, 2H, H-2′and H-6′), 6.60 (d, *J* = 7.9 Hz, 1H, H-5), 6.54 (d, *J* = 2.1 Hz, 1H, H-2), 6.39 (dd, *J* = 8.0, 2.1 Hz, 1H, H-6), 2.82 (p, *J* = 6.9 Hz, 1H, Ph′-CH), 2.53 (d, *J* = 6.7 Hz, 2H, Ph-CH_2), 2.41 (t, *J* = 6.9 Hz, 2H, Ph′-CH_2), 1.57–1.44 (m, 4H, $CH_2\underline{CH_2}\underline{CH_2}CH_2$), 1.17 (d, *J* = 6.9 Hz, 6H, 2×CH_3); ^{13}C NMR (150 MHz,

$CDCl_3$) δ 146.17, 143.29, 141.22, 139.92, 135.99, 128.32 (2C), 126.30 (2C), 120.89, 115.53, 115.26, 35.40, 35.10, 33.70, 31.23, 31.06, 24.10 (2C); ESI-MS *m/z* calcd for $C_{19}H_{23}O_2$ [M - H]$^-$ 283.2, found 283.3.

*4.1.7.4. 4-(4-(4-Hydroxyphenyl)butyl)benzene-1,2-diol (**WA4**).* White solid, yield 51%, mp 121–123 °C, R_f = 0.56 (DCM/MeOH = 10:1); ^{1}H NMR (400 MHz, DMSO-d_6) δ 9.09 (s, 1H, OH), 8.67 (s, 1H, OH), 8.57 (s, 1H, OH), 6.95 (d, *J* = 1.9 Hz, 1H, H-2′), 6.93 (d, *J* = 2.2 Hz, 1H, H-6′), 6.65 (d, *J* = 1.9 Hz, 1H, H-3′), 6.63 (d, *J* = 2.1 Hz, 1H, H-5′), 6.59 (d, *J* = 7.9 Hz, 1H, H-5), 6.52 (d, *J* = 2.1 Hz, 1H, H-2), 6.38 (dd, *J* = 8.0, 2.1 Hz, 1H, H-6), 2.48–2.42 (m, 2H, Ph-CH_2), 2.42–2.36 (m, 2H, Ph′-CH_2), 1.48 (m, *J* = 3.4 Hz, 4H, $CH_2\underline{CH_2}\underline{CH_2}CH_2$); ^{13}C NMR (150 MHz, DMSO-d_6) δ 155.64, 145.37, 143.50, 133.50, 132.74, 129.50 (2C), 119.27, 116.09, 115.83, 115.42 (2C), 34.82, 34.61, 31.39, 31.28; ESI-MS *m/z* calcd for $C_{16}H_{17}O_3$ [M - H]$^-$ 257.1, found 257.2.

*4.1.7.5. 4-(4-(2-Hydroxyphenyl)butyl)benzene-1,2-diol (**WA5**).* White solid, yield 51%, mp 134–136 °C, R_f = 0.59 (DCM/MeOH = 10:1); ^{1}H NMR (400 MHz, DMSO-d_6) δ 9.16 (s, 1H, OH), 8.67 (s, 1H, OH), 8.56 (s, 1H, OH), 7.03–6.93 (m, 2H, H-6′ and H-4′), 6.74 (d, *J* = 7.9 Hz, 1H, H-3′), 6.68 (dd, *J* = 7.9, 6.7 Hz, 1H, H-5′), 6.59 (d, 1H, H-5), 6.53 (d, *J* = 2.0 Hz, 1H, H-2), 6.39 (dd, *J* = 7.9, 2.0 Hz, 1H, H-6), 2.52 (d, J = 6.6 Hz, 2H, Ph-CH_2), 2.39 (t, *J* = 6.7 Hz, 2H, Ph′-CH_2), 1.49 (m, *J* = 3.6 Hz, 4H, $CH_2\underline{CH_2}\underline{CH_2}CH_2$); ^{13}C NMR (100 MHz, DMSO-d_6) δ 155.47, 145.37, 143.49, 133.63, 130.19, 128.83, 127.03, 119.30, 119.23, 116.14, 115.84, 115.31, 34.96, 31.66, 29.91, 29.52; HRMS *m/z* calcd for $C_{16}H_{17}O_3$ [M - H]$^-$ 257.1256, found 257.1195.

*4.1.7.6. 4,4'-(Butane-1,4-diyl)bis(benzene-1,2-diol) (**WA6**).* Light brown solid, yield 56 %, mp 141–142 °C, R_f = 0.52 (DCM/MeOH = 10:1); ^{1}H NMR (400 MHz, DMSO-d_6) δ 8.56 (s, 4H, 4×OH), 6.59 (d, *J* = 8.0 Hz, 2H, H-5 and H-5′), 6.53 (d, *J* = 2.1 Hz, 2H, H-2 and H-2′), 6.39 (dd, *J* = 8.0, 2.1 Hz, 2H, H-6 and H-6′), 2.45–2.33 (m, 4H, Ph-CH_2 and Ph′-CH_2), 1.47 (h, *J* = 3.4 Hz, 4H, $CH_2\underline{CH_2}\underline{CH_2}CH_2$); ^{13}C NMR (100 MHz, DMSO-d_6) δ 145.37 (2C), 143.49 (2C), 133.52 (2C), 119.28 (2C), 116.09 (2C), 115.83 (2C), 34.85 (2C), 31.31 (2C); ESI-MS *m/z* calcd for $C_{16}H_{17}O_4$ [M - H]$^-$ 273.1, found 273.3.

*4.1.7.7. 5-(4-(3,4-Dihydroxyphenyl)butyl)benzene-1,2,3-triol (**WA7**).* White solid, yield 65%, mp 192–193 °C, R_f = 0.14 (DCM/MeOH = 10:1); ^{1}H NMR (400 MHz, DMSO-d_6) δ 8.68 (s, 1H, OH), 8.60 (s, 2H, 2×OH), 8.57 (s, 1H, OH), 7.78 (s, 1H, OH), 6.60 (d, *J* = 7.9 Hz, 1H, H-5), 6.53 (d, *J* = 2.1 Hz, 1H, H-2), 6.39 (dd, *J* = 8.0, 2.1 Hz, 1H, H-6), 6.05 (s, 2H, H-2′ and H-6′), 2.38 (d, *J* = 7.0 Hz, 2H, Ph′-CH_2), 2.32 (d, *J* = 7.1 Hz, 2H, Ph-CH_2), 1.45 (m, *J* = 3.9 Hz, 4H, $CH_2\underline{CH_2}\underline{CH_2}CH_2$); ^{13}C NMR (100 MHz, DMSO-d_6) δ 146.34 (2C), 145.38, 143.49, 133.56, 132.85, 131.17, 119.30, 116.12, 115.86, 107.45 (2C), 35.14, 34.88, 31.29, 31.15; HRMS *m/z* calcd for $C_{16}H_{17}O_5$ [M - H]$^-$ 289.1154, found 289.1087.

*4.1.7.8. 4-(4-(4-Fluorophenyl)butyl)benzene-1,2-diol (**WA8**).* White solid, yield 64%, mp 70–72 °C, R_f = 0.53 (DCM/MeOH = 10:1); ^{1}H NMR (400 MHz, DMSO-d_6) δ 8.68 (s, 1H, OH), 8.58 (s, 1H, OH), 7.24–7.15 (m, 2H, H-2′ and H-6′), 7.11–7.03 (m, 2H, H-3′ and H-5′), 6.60 (d, *J* = 7.9 Hz, 1H, H-5), 6.53 (d, *J* = 2.1 Hz, 1H, H-2), 6.39 (dd, *J* = 7.9, 2.1 Hz, 1H, H-6), 2.56 (t, *J* = 7.1 Hz, 2H, Ph-CH_2), 2.40 (t, *J* = 7.1 Hz, 2H, Ph′-CH_2), 1.56–1.43 (m, 4H, $CH_2\underline{CH_2}\underline{CH_2}CH_2$); ^{13}C NMR (100 MHz, $CDCl_3$) δ 162.37, 159.95, 143.36, 141.28, 138.13, 135.81, 129.73(2C), 120.82, 115.30, 115.07 (2C), 35.05, 34.97, 31.09, 31.05; ESI-MS *m/z* calcd for $C_{18}H_{17}O_4F_4$ [M + CF_3COO]$^-$ 373.1, found 373.2.

*4.1.7.9. 4-(4-(4-Chlorophenyl)butyl)benzene-1,2-diol (**WA9**).* White solid, yield 63%, mp 93–95 °C, R_f = 0.62 (DCM/MeOH = 10:1); ^{1}H NMR (600 MHz, DMSO-d_6) δ 8.68 (s, 1H, OH), 8.58 (s, 1H, OH), 7.73 (d, *J* = 8.3 Hz, 2H, H-2′ and H-6′), 7.43 – 7.37 (m, 2H, H-3′ and H-5′), 6.60 (d, *J* = 8.0 Hz, 1H, H-5), 6.52 (d, *J* = 2.1 Hz, 1H, H-2), 6.39 (dd, *J* = 8.0, 2.1 Hz, 1H, H-6), 2.67 (t, *J* = 7.6 Hz, 2H, Ph-CH_2), 2.41 (t, *J* = 7.5 Hz, 2H, Ph′-CH_2), 1.59–1.52 (m, 2H, $CH_2\underline{CH_2}CH_2CH_2$), 1.51–1.45 (m, 2H, $CH_2CH_2\underline{CH_2}CH_2$); ^{13}C NMR (150 MHz, DMSO-d_6) δ 145.39, 143.52, 142.72, 133.43, 128.72 (2C), 128.67 (2C), 126.05, 119.27, 116.10, 115.84, 35.46, 34.79, 31.31, 31.09; ESI-MS *m/z* calcd for $C_{16}H_{16}ClO_2$ [M – H]$^-$ 275.1, found 275.5.

*4.1.7.10. 4-(4-(4-Bromophenyl)butyl)benzene-1,2-diol (**WA10**).* White solid, yield 54%, mp 78–80 °C, R_f = 0.60 (DCM/MeOH = 10:1). ^{1}H NMR (400 MHz, DMSO-d_6) δ 8.68 (s, 1H, OH), 8.58 (s, 1H, OH), 7.23–7.16 (m, 2H, H-2′ and H-6′), 7.11–7.03 (m, 2H, H-3′ and H-5′), 6.60 (d, *J* = 7.9 Hz, 1H, H-5), 6.53 (d, *J* = 2.1 Hz, 1H, H-2), 6.39 (dd, *J*

= 7.9, 2.1 Hz, 1H, H-6), 2.56 (t, *J* = 7.1 Hz, 2H, Ph-CH_2), 2.40 (t, *J* = 7.1 Hz, 2H, Ph′-CH_2), 1.56–1.45 (m, 4H, $CH_2\underline{CH_2}\underline{CH_2}CH_2$). ^{13}C NMR (100 MHz, $CDCl_3$) δ 143.30, 142.64, 141.25, 135.93, 128.46 (2C), 128.30 (2C), 125.68, 120.89, 115.56, 115.31, 35.84, 35.09, 31.17, 31.02. ESI-MS *m/z* calcd for $C_{18}H_{17}BrO_4F_3$ [M + CF_3COO]$^-$ 433.0, found 433.4.

*4.1.7.11. 4-(4-(Tert-butyl)phenyl)butyl)benzene-1,2-diol (**WA11**).* White solid, yield 76%, mp 88–90 °C, R_f = 0.19 (DCM/MeOH = 30:1); ^{1}H NMR (600 MHz, DMSO-d_6) δ 8.66 (s, 1H, OH), 8.57 (s, 1H, OH), 7.29–7.24 (m, 2H, H-3′ and H-5′), 7.09 (d, *J* = 8.2 Hz, 2H, H-2′ and H-6′), 6.60 (d, *J* = 7.9 Hz, 1H, H-5), 6.54 (d, *J* = 2.1 Hz, 1H, H-2), 6.40 (dd, *J* = 8.0, 2.1 Hz, 1H, H-6), 2.53 (t, *J* = 7.2 Hz, 2H, Ph-CH_2), 2.41 (t, *J* = 7.1 Hz, 2H, Ph′-CH_2), 1.57–1.47 (m, 4H, $CH_2\underline{CH_2}\underline{CH_2}CH_2$), 1.26 (s, 9H, 3×$CH_3$); ^{13}C NMR (100 MHz, $CDCl_3$) δ 148.45, 143.28, 141.22, 139.55, 135.99, 128.08 (2C), 125.17 (2C), 120.90, 115.55, 115.28, 35.29, 35.11, 34.37, 31.46(3C), 31.28, 31.01; ESI-MS *m/z* calcd for $C_{21}H_{27}O_4$ [M + HCOO]$^-$ 343.2, found 343.5.

*4.1.7.12. 4-(4-(4-Aminophenyl)butyl)benzene-1,2-diol (**WA12**).* White solid, yield 24%, mp 126–128 °C, R_f = 0.53 (DCM/MeOH = 10:1); ^{1}H NMR (400 MHz, DMSO-d_6) δ 8.67 (s, 1H, OH), 8.55 (s, 1H, OH), 6.83–6.77 (m, 2H, H-2′ and H-6′), 6.59 (d, *J* = 7.9 Hz, 1H, H-5), 6.52 (d, *J* = 2.1 Hz, 1H, H-2), 6.48–6.43 (m, 2H, H-3′ and H-5′), 6.38 (dd, *J* = 7.9, 2.1 Hz, 1H, H-6), 4.79 (s, 2H, NH_2), 2.39 (h, *J* = 2.9 Hz, 4H, 2×Ph-CH_2), 1.46 (m, *J* = 3.6 Hz, 4H, $CH_2\underline{CH_2}\underline{CH_2}CH_2$); ^{13}C NMR (100 MHz, DMSO-d_6) δ 148.15, 145.36, 143.48, 133.55, 129.69, 129.12 (2C), 119.26, 116.09, 115.82, 112.27 (2C), 34.87, 34.65, 31.55, 31.31; ESI-MS *m/z* calcd for $C_{16}H_{20}NO_2$ [M + H]$^+$ 258.1, found 258.2.

*4.1.7.13. 4-(4-(Thiophen-2-yl)butyl)benzene-1,2-diol (**WB1**).* White solid, yield 64%, mp 151–153 °C, R_f = 0.23 (DCM/MeOH = 30:1); ^{1}H NMR (400 MHz, DMSO-d_6) δ 8.67 (s, 1H, OH), 8.57 (s, 1H, OH), 8.48 (dd, *J* = 5.2, 1.7 Hz, 1H, H-3′), 7.74 (td, *J* = 7.6, 1.8 Hz, 1H, H-5′), 7.28 (d, *J* = 7.8 Hz, 1H, H-6′), 7.23 (ddd, *J* = 7.5, 4.9, 1.1 Hz, 1H, H-4′), 6.60 (d, *J* = 8.0 Hz, 1H, H-5), 6.53 (d, *J* = 2.0 Hz, 1H, H-2), 6.39 (dd, *J* = 8.0, 2.1 Hz, 1H, H-6), 2.77–2.70 (m, 2H, Py-CH_2), 2.41 (t, *J* = 7.5 Hz, 2H, Ph-CH_2), 1.65 (ddd, *J* = 15.4, 8.8, 6.7 Hz, 2H, $CH_2\underline{CH_2}CH_2CH_2$), 1.51 (h, *J* = 7.3, 6.8 Hz, 2H, $CH_2CH_2\underline{CH_2}CH_2$); ^{13}C NMR (150 MHz, DMSO-d_6) δ 145.52, 143.81, 134.69, 134.05, 132.49, 131.97, 130.86, 129.16, 119.36, 116.09, 115.93, 35.77, 28.59, 28.11, 24.03; ESI-MS *m/z* calcd for $C_{15}H_{18}NO_2$ [M + H]$^+$ 244.1, found 244.4.

*4.1.7.14. 4-(4-(Tetrahydrofuran-2-yl)butyl)benzene-1,2-diol (**WB2**).* Yellow oil, yield 45%, R_f = 0.30 (DCM/MeOH = 30:1); ^{1}H NMR (400 MHz, DMSO-d_6) δ 8.62 (s, 2H, OH), 6.61 (d, *J* = 7.9 Hz, 1H, H-5), 6.55 (d, *J* = 2.1 Hz, 1H, H-2), 6.41 (dd, *J* = 8.0, 2.1 Hz, 1H, H-6), 4.23 (tt, *J* = 8.5, 4.3 Hz, 1H, $\underline{CH}OCH_2$), 3.60–3.50 (m, 2H, CHO$\underline{CH_2}$), 2.39 (t, *J* = 7.2 Hz, 2H, Ph-CH_2), 1.95 (dd, *J* = 27.0, 15.3, 10.4, 7.5, 5.6 Hz, 4H, $OCH_2\underline{CH_2}\underline{CH_2}$), 1.81 (qd, *J* = 8.5, 4.1 Hz, 2H, $PhCH_2CH_2CH_2\underline{CH_2}$), 1.60–1.19 (m, 4H, $PhCH_2\underline{CH_2}\underline{CH_2}CH_2$); ^{13}C NMR (150 MHz, $CDCl_3$) δ 143.40, 141.34, 135.62, 120.79, 115.49, 115.31, 56.89, 39.11, 37.34, 35.02, 33.06, 30.91, 30.60, 27.12; ESI-MS *m/z* calcd for $C_{14}H_{24}NO_3$ [M + NH_4]$^+$ 254.1, found 254.3.

*4.1.7.15. 4-(4-(Pyridin-4-yl)butyl)benzene-1,2-diol (**WB3**).* White solid, yield 42%, mp 134–136 °C, R_f = 0.42 (DCM/MeOH = 10:1); ^{1}H NMR (400 MHz, DMSO-d_6) δ 8.69 (s, 1H, OH), 8.59 (s, 1H, OH), 8.43 (d, *J* = 5.5 Hz, 2H, H-3′ and H-5′), 7.24–7.16 (m, 2H, H-2′ and H-6′), 6.60 (d, *J* = 7.9 Hz, 1H, H-5), 6.53 (d, *J* = 2.1 Hz, 1H, H-2), 6.40 (dd, *J* = 8.0, 2.1 Hz, 1H, H-6), 2.59 (t, *J* = 7.4 Hz, 2H, Py-CH_2), 2.41 (t, *J* = 7.3 Hz, 2H, Ph-CH_2), 1.61–1.44 (m, 4H, $CH_2\underline{CH_2}\underline{CH_2}CH_2$); ^{13}C NMR (100 MHz, $CDCl_3$) δ 153.23, 148.22 (2C), 144.57, 142.67, 134.21, 124.53 (2C), 119.99, 115.12, 114.92, 35.12, 34.91, 30.84, 29.44; ESI-MS *m/z* calcd for $C_{15}H_{18}NO_2$ [M + H]$^+$ 244.1, found 244.3.

*4.1.7.16. 4-(4-([1,1'-Biphenyl]-4-yl)butyl)benzene-1,2-diol (**WB4**).* White solid, yield 86%, mp 128–130 °C, R_f = 0.27 (DCM/MeOH = 30:1); ^{1}H NMR (400 MHz, DMSO-d_6) δ 8.68 (s, 1H, OH), 8.58 (s, 1H, OH), 7.64 (d, *J* = 1.5 Hz, 1H, H-2″), 7.62 (t, *J* = 1.2 Hz, 1H, H-6″), 7.57 (d, *J* = 1.9 Hz, 1H, H-3′), 7.55 (d, *J* = 1.9 Hz, 1H, H-5′), 7.44 (t, *J* = 7.7 Hz, 2H, H-2″ and H-6″), 7.37–7.31 (m, 1H, H-4″), 7.26 (d, *J* = 8.0 Hz, 2H, H-2′ and H-6′), 6.60 (d, *J* = 7.9 Hz, 1H, H-5), 6.55 (d, *J* = 2.0 Hz, 1H, H-2), 6.41 (dd, *J* = 8.0, 2.1 Hz, 1H, H-6), 2.62 (t, *J* = 7.2 Hz, 2H, Ph′-CH_2), 2.43 (t, *J* = 7.1 Hz, 2H, Ph-CH_2), 1.56 (ddd, *J* = 20.2, 11.5, 5.4 Hz, 4H,$CH_2\underline{CH_2}\underline{CH_2}CH_2$); ^{13}C NMR (150 MHz, DMSO-d_6) δ 145.40, 143.54, 142.04, 140.60, 138.02, 133.43, 129.33 (4C), 127.57, 127.00 (2C), 126.93 (2C), 119.30, 116.13, 115.85,

35.06, 34.82, 31.34, 31.01; ESI-MS *m/z* calcd for $C_{22}H_{26}O_2N$ $[M + NH_4]^+$ 336.2, found 336.6.

*4.1.7.17. 4-(4,4-Diphenylbutyl)benzene-1,2-diol (**WB5**).* Yellow oil, yield 57%, R_f = 0.38 (DCM/MeOH = 30:1); ^{1}H NMR (400 MHz, DMSO-d_6) δ 8.67 (s, 1H, OH), 8.56 (s, 1H, OH), 7.31–7.22 (m, 8H, Ar-H), 7.14 (dd, *J* = 6.0, 3.1 Hz, 2H, Ar-H), 6.58 (d, *J* = 7.9 Hz, 1H, H-5), 6.49 (d, *J* = 2.0 Hz, 1H, H-2), 6.35 (dd, *J* = 8.0, 2.0 Hz, 1H, H-6), 3.93 (t, *J* = 7.9 Hz, 1H, Ph-CH-Ph), 2.41 (t, *J* = 7.6 Hz, 2H, Ph-CH_2), 1.99 (q, *J* = 7.9 Hz, 2H, $CH_2CH_2\underline{CH_2}CHPh_2$), 1.39 (td, *J* = 7.6, 7.1, 3.7 Hz, 2H, $CH_2\underline{CH_2}CH_2CHPh_2$); ^{13}C NMR (100 MHz, $CDCl_3$) δ 143.30, 141.72, 141.23, 141.13, 138.63, 135.90, 128.84 (2C), 128.71 (2C), 128.68, 127.02 (2C), 126.99 (2C), 120.87, 115.51, 115.26, 35.45, 35.08, 31.18, 30.96; ESI-MS *m/z* calcd for $C_{24}H_{22}O_4F_3$ $[M + CF_3COO]^-$ 431.2, found 431.6.

*4.1.7.18. 4-(4-(Naphthalen-1-yl)butyl)benzene-1,2-diol (**WB6**).* White solid, yield 34%, mp 136–138 °C, R_f = 0.59 (DCM/MeOH = 10:1); ^{1}H NMR (400 MHz, DMSO-d_6) δ 8.67 (s, 1H, OH), 8.57 (s, 1H, OH), 8.03 (dd, *J* = 7.8, 1.6 Hz, 1H, H-8′), 7.93–7.85 (m, 1H, H-5′), 7.75 (d, *J* = 8.1 Hz, 1H, H-4′), 7.51 (pd, 2H, H-6′ and H-3′), 7.40 (dd, *J* = 8.1, 7.0 Hz, 1H, H-7′), 7.33 (dd, *J* = 7.0, 1.3 Hz, 1H, H-2′), 6.61 (d, *J* = 7.9 Hz, 1H, H-5), 6.56 (d, *J* = 2.1 Hz, 1H, H-2), 6.42 (dd, *J* = 8.0, 2.1 Hz, 1H, H-6), 3.04 (t, *J* = 7.2 Hz, 2H, Ar′-CH_2), 2.45 (t, *J* = 7.1 Hz, 2H, Ph-CH_2), 1.69–1.58 (m, 4H, $CH_2\underline{CH_2}\underline{CH_2}CH_2$); ^{13}C NMR (150 MHz, DMSO-d_6) δ 145.41, 143.53, 138.91, 133.91, 133.40, 131.81, 129.01, 126.72, 126.35, 126.31, 126.03, 125.94, 124.22, 119.31, 116.15, 115.84, 34.80, 32.56, 31.67, 30.55; ESI-MS *m/z* calcd for $C_{22}H_{20}O_4F_3$ $[M + CF_3COO]^-$ 405.1, found 405.6.

*4.1.7.19. 4-(4-(6-Hydroxynaphthalen-2-yl)butyl)benzene-1,2-diol (**WB7**).* White solid, yield 51%, mp 147–149 °C, R_f = 0.55 (DCM/MeOH = 10:1); ^{1}H NMR (400 MHz, DMSO-d_6) δ 9.58 (s, 1H, Ar′-OH), 8.67 (s, 1H, Ph-OH), 8.57 (s, 1H, Ph-OH), 7.66 (d, *J* = 8.7 Hz, 1H, H-8′), 7.58 (d, *J* = 8.4 Hz, 1H, H-4′), 7.51 (d, *J* = 1.6 Hz, 1H, H-5′), 7.23 (dd, *J* = 8.4, 1.7 Hz, 1H, H-3′), 7.06 (d, *J* = 2.4 Hz, 1H, H-7′), 7.03 (dd, 1H, H-2′), 6.59 (d, *J* = 7.9 Hz, 1H, H-5), 6.53 (d, *J* = 2.1 Hz, 1H, H-2), 6.39 (dd, *J* = 8.0, 2.1 Hz, 1H, H-6), 2.68 (t, *J* = 7.4 Hz, 2H, Ar′-CH_2), 2.42 (t, *J* = 7.4 Hz, 2H, Ph-CH_2), 1.57 (dq, *J* = 31.9, 7.5 Hz, 4H, $CH_2\underline{CH_2}\underline{CH_2}CH_2$); ^{13}C NMR (150 MHz, DMSO-d_6) δ 155.11, 145.39, 143.52, 136.82, 133.46, 133.42, 129.17, 128.28, 127.99, 126.39, 126.33, 119.28, 118.94, 116.11, 115.84, 108.95, 35.39, 34.85, 31.36, 31.03; ESI-MS *m/z* calcd for $C_{21}H_{21}O_4$ $[M + HCOO]^-$ 353.1, found 353.3.

*4.1.7.20. 4-(4-(1-Methyl-1H-indol-3-yl)butyl)benzene-1,2-diol (**WB8**).* Yellow oil, yield 44%, R_f = 0.24 (DCM/MeOH = 30:1); ^{1}H NMR (400 MHz, DMSO-d_6) δ 8.67 (s, 1H, OH), 8.57 (s, 1H, OH), 7.48 (dt, *J* = 7.8, 1.0 Hz, 1H, H-6′), 7.35 (dd, *J* = 8.2, 0.9 Hz, 1H, H-7′), 7.11 (ddd, *J* = 8.2, 7.0, 1.2 Hz, 1H, I H-4′), 7.04 (s, 1H, H-2′), 6.98 (ddd, *J* = 7.9, 7.0, 1.0 Hz, 1H, H-5′), 6.60 (d, *J* = 7.9 Hz, 1H, H-5), 6.54 (d, *J* = 2.1 Hz, 1H, H-2), 6.40 (dd, *J* = 8.0, 2.1 Hz, 1H, H-6), 3.71 (s, 3H, CH_3), 2.66 (d, *J* = 7.3 Hz, 2H, Ph-CH_2), 2.43 (t, *J* = 7.2 Hz, 2H, Ar′-CH_2), 1.59 (dq, *J* = 21.8, 7.9 Hz, 4H, $CH_2\underline{CH_2}\underline{CH_2}CH_2$); ^{13}C NMR (150 MHz, $CDCl_3$) δ 143.32, 141.32, 137.04, 135.97, 127.96, 126.12, 121.38, 120.87, 120.85, 119.11, 118.45, 115.50, 115.20, 109.13, 35.09, 32.56, 31.40, 29.88, 24.94; ESI-MS *m/z* calcd for $C_{19}H_{22}NO_2$ $[M + H]^+$ 296.2, found 296.3.

*4.1.7.21. 4-(4-(1-Isopentyl-1H-indol-3-yl)butyl)benzene-1,2-diol (**WB9**).* Yellow oil, yield 44%, R_f = 0.13 (DCM/MeOH = 10:1); ^{1}H NMR (400 MHz, DMSO-d_6) δ 8.65 (s, 1H, OH), 8.56 (s, 1H, OH), 7.48 (dt, *J* = 7.9, 1.0 Hz, 1H, H-6′), 7.37 (dt, *J* = 8.2, 0.9 Hz, 1H, H-7′), 7.13–7.06 (m, 2H, H-4′ and H-2′), 6.96 (ddd, *J* = 7.9, 7.0, 1.0 Hz, 1H, H-5′), 6.59 (d, *J* = 7.9 Hz, 1H, H-5), 6.54 (d, *J* = 2.1 Hz, 1H, H-2), 6.40 (dd, *J* = 8.0, 2.1 Hz, 1H, H-6), 4.10 (t, *J* = 7.3 Hz, 2H, $N\underline{CH_2}CH_2$), 2.67 (t, *J* = 7.2 Hz, 2H, Ph-CH_2), 2.43 (t, *J* = 7.3 Hz, 2H, Ar′-CH_2), 1.70–1.58 (m, 4H, $CH_2\underline{CH_2}\underline{CH_2}CH_2$), 1.58–1.38 (m, 2H, $NCH_2\underline{CH_2}$), 1.09 (t, *J* = 7.0 Hz, 1H, $\underline{CH}(CH_3)_2$), 0.90 (d, *J* = 6.6 Hz, 6H, 2×CH_3); ^{13}C NMR (150 MHz, $CDCl_3$) δ 143.26, 141.25, 136.27, 136.04, 128.01, 124.90, 121.20, 120.87, 119.32, 119.18, 118.34, 115.51, 115.21, 109.26, 44.34, 39.12, 35.06, 31.39, 29.81, 25.79, 25.00, 22.49 (2C); ESI-MS *m/z* calcd for $C_{23}H_{30}NO_2$ $[M + H]^+$ 352.2, found 352.9.

*4.1.7.22. 4-(4-(3,4,5,6-Tetrahydroanthracen-9-yl)butyl)benzene-1,2-diol (**WB10**).* White solid, yield 65%, mp 158–160 °C, R_f = 0.25 (DCM/MeOH = 30:1); ^{1}H NMR (400 MHz, DMSO-d_6) δ 8.68 (s, 1H, OH), 8.59 (s, 1H, OH), 7.94–7.89 (m, 1H, H-6′), 7.72 (dd, *J* = 7.5, 2.0 Hz, 1H, H-2′), 7.45 (s, 1H, H-10′), 7.37 (td, *J* = 7.2, 1.6 Hz, 2H, H-3′ and H-9′), 6.62 (d, *J* = 7.9 Hz, 1H, H-5), 6.54 (d, *J* = 2.1 Hz, 1H, H-2), 6.45 (dd, *J* = 8.0, 2.1 Hz, 1H, H-6), 3.02 – 2.95 (m, 2H, Ar′-CH_2), 2.90 (t, *J* = 6.3 Hz, 2H, CH_2), 2.85 (t, *J* = 6.5 Hz, 2H, CH_2), 2.48 (d, *J* = 7.4 Hz, 2H, Ph-CH_2), 1.81 (q,

J = 6.6, 6.1 Hz, 2H, $CH_2CH_2\underline{CH_2}CH_2$), 1.78–1.65 (m, 4H, 2×$CH_2$), 1.55–1.43 (m, 2H, $CH_2\underline{CH_2}CH_2CH_2$); ^{13}C NMR (150 MHz, DMSO-d_6) δ 145.43, 143.54, 136.13, 135.90, 133.36, 133.34, 132.20, 130.64, 128.08, 125.57, 125.37, 124.99, 123.88, 119.34, 116.17, 115.84, 34.79, 32.04, 30.70, 29.69, 27.69, 26.76, 23.66, 22.81; ESI-MS *m/z* calcd for $C_{26}H_{26}O_4F_3$ [M + CF_3COO] $^-$ 459.2, found 459.6.

*4.1.7.23. 4-(4-(Pyren-4-yl)butyl)benzene-1,2-diol (**WB11**).* White solid, yield 57%, mp 66–68 °C, R_f = 0.23 (DCM/MeOH = 30:1); ^{1}H NMR (400 MHz, DMSO-d_6) δ 8.68 (s, 1H, OH), 8.58 (s, 1H, OH), 8.32 (d, *J* = 9.3 Hz, 1H, H-8′), 8.27 (dd, *J* = 7.6, 2.4 Hz, 2H, H-4′ and H-6′), 8.20 (dd, *J* = 8.5, 5.0 Hz, 2H, H-2′ and H-7′), 8.12 (d, *J* = 1.6 Hz, 2H, H-4′ and H-9′), 8.05 (t, *J* = 7.6 Hz, 1H, H-10′), 7.93 (d, *J* = 7.8 Hz, 1H, H-3′), 6.60 (d, *J* = 7.9 Hz, 1H, H-5), 6.57 (d, *J* = 2.2 Hz, 1H, H-2), 6.42 (dd, *J* = 8.0, 2.1 Hz, 1H, H-6), 3.21 (d, *J* = 7.4 Hz, 2H, Ar′-CH_2), 2.47 (d, *J* = 7.7 Hz, 2H, Ph-CH_2), 1.84-1.64 (m, 4H, $CH_2\underline{CH_2}\underline{CH_2}CH_2$); ^{13}C NMR (100 MHz, DMSO-d_6) δ 145.43, 143.55, 137.53, 133.42, 131.37, 130.89, 129.65, 128.49, 127.92, 127.61, 126.88, 126.57, 125.94, 125.36, 125.18, 124.70, 124.65, 123.98, 123.06, 119.34, 116.18, 115.87, 34.85, 32.96, 31.64, 31.58; HRMS *m/z* calcd for $C_{26}H_{21}O_2$ [M – H] $^-$ 365.1620, found 365.1558.

*4.1.8. (E)-1,3-Bis(3,4-dimethoxyphenyl)prop-2-en-1-one (**9**)*

To a solution of 3,4-dimethoxybenzaldehyde (**1**) (3.00 g, 18.05 mmol) and 3,4-dimethoxyacetophenone (**8**) (3.25 g, 18.05 mmol) in 45 mL of ethanol (EtOH) was added NaOH (0.80 g, 19.86 mmol). The solution was allowed to warm to 75 °C and stirred for 6 h. After concentrating under reduced pressure, the residue was poured in water (30 mL) and extracted with EtOAc (3 × 20 mL). The combined organic extracts were dried over anhydrous Na_2SO_4, filtered, and concentrated in vacuo. The residue was purified by flash column chromatography (petroleum ether/EtOAc) to afford 5.30 g of **9** as a yellow solid in a yield of 90%. mp: 110–112 °C.

*4.1.9. 1,3-Bis(3,4-dimethoxyphenyl)propan-1-one (**10**)*

The title compound **10** was synthesized in a yield of 97% in a manner similar to the synthesis of **7**.

*4.1.10. 1,3-Bis(3,4-dimethoxyphenyl)propan-1-ol (**11**)*

$NaBH_4$ (0.29 g, 7.67 mmol) was added to a solution of **10** (1.95 g, 5.90 mmol) in MeOH (30 mL), and the resulting mixture was stirred at 0 °C for 1 h. Water (20 mL) was added to the mixture, which was extracted with EtOAc (3 × 20 mL). The organic phase was dried over anhydrous Na_2SO_4, filtered, and concentrated in vacuo. The residue was purified using flash column chromatography with elution system of petroleum ether/EtOAc to generate 1.89 g of **11** as yellow oil, in a yield of 96%.

*4.1.11. 4,4'-(Prop-1-ene-1,3-diyl)bis(1,2-dimethoxybenzene)(**12**)*

To a solution of **11** (1.00 g, 3.01 mmol) in dioxane (25 mL) was added 7-8 drops of H_2SO_4, and the reaction mixture was refluxed for 5 h before pouring into iced water (20 mL). The mixture was extracted with EtOAc (3 × 20 mL). Then washed with saturated $NaHCO_3$ and brine, dried with anhydrous Na_2SO_4, and concentrated in vacuo to afford 0.64 g yellow oil in a yield of 68%.

*4.1.12. 1,3-Bis(3,4-dimethoxyphenyl)propane (**13**)*

The compound **13** was synthesized in a manner similar to the synthesis of **7**, white solid in a yield of 82%. mp: 62-63 °C.

*4.1.13. 4,4'-(Propane-1,3-diyl)bis(benzene-1,2-diol) (**WC1**)*

The target compound **WC1** was synthesized in a manner similar to the synthesis of **WA1-WA12**, The desired product **WC1** was obtained as white solid in a yield of 71%. mp: 115–117 °C, R_f = 0.50 (DCM/MeOH = 10:1); ^{1}H NMR (400 MHz, DMSO-d_6) δ 8.69 (s, 2H, 2 × OH), 8.58 (s, 2H, 2 × OH), 6.61 (d, *J* = 7.9 Hz, 2H, H-5 and H-5′), 6.55 (d, *J* = 2.0 Hz, 2H, H-2 and H-2′), 6.41 (dd, *J* = 8.0, 2.0 Hz, 2H, H-6 and H-6′), 2.38 (t, *J* = 7.6 Hz, 4H, 2 × Ph-CH_2), 1.70 (p, *J* = 7.6 Hz, 2H, $CH_2\underline{CH_2}CH_2$); ^{13}C NMR (100 MHz, DMSO-d_6) δ 145.43 (2C), 143.53 (2C), 133.38 (2C), 119.30 (2C), 116.11 (2C), 115.90 (2C), 34.48 (2C), 33.65; HRMS *m/z* calcd for $C_{15}H_{15}O_4$ [M - H] $^-$ 259.1049, found 259.1018.

*4.1.14. (1E,4E)-1,5-Bis(3,4-dimethoxyphenyl)penta-1,4-dien-3-one (**14**)*

To a solution of 3,4-dimethoxybenzaldehyde (1) (3.00 g, 18.05 mmol) and acetone (0.87 g, 9.03 mmol) in EtOH-H_2O

mixture (4:1, 30 mL) at 0 °C was added NaOH (1.81 g, 45.18 mmol) slowly. the resulting solution was raised to room temperature and stirred for 1 h. the precipitate was filtered off, washed with water, and recrystallized from EtOH to give a solid (2.78 g, 87%). mp: 84–86 °C.

*4.1.15. 1,5-Bis(3,4-dimethoxyphenyl)pentan-3-one (**15**)*

The title compound **15** was synthesized in a manner similar to the synthesis of **7**. White solid, yield 95%, mp: 83–85°C.

*4.1.16. 1,5-Bis(3,4-dimethoxyphenyl)pentane(**16**)*

Hydrazine hydrate (0.56 g, 11.14 mmol) was added dropwise to a stirring mixture of **15** (2.00 g, 5.57 mmol) and KOH (0.78 g, 13.93 mmol) in diethylene glycol (30 mL). After the addition was complete, the resulting mixture was heated at 105°C for 5 h under a nitrogen atmosphere before pouring into water (100 mL).The resultant mixture was extracted with EtOAc (3 × 30 mL). The combined organic extracts were washed with water and brine, dried over anhydrous Na_2SO_4, and concentrated in vacuo. The residue was purified by flash column chromatography (petroleum ether/EtOAc) to give 0.56 g of **16** as a white solid in a yield of 96%. mp: 56–58 °C.

*4.1.17. 4,4'-(Pentane-1,5-diyl)bis(benzene-1,2-diol) (**WC2**)*

The title compound **WC2** was prepared according to the procedure depicted for compounds **WA1-WA12**. The desired product **WC2** was obtained as a white solid in a yield of 47%. mp: 129–131 °C, R_f = 0.53 (DCM/MeOH = 10:1); ^{1}H NMR (400 MHz, DMSO-*d6*) δ 8.66 (s, 2H, 2 × OH), 8.56 (s, 2H, 2 × OH), 6.60 (d, J = 7.9 Hz, 2H, H-5 and H-5′), 6.53 (d, J = 2.1 Hz, 2H, H-2 and H-2′), 6.39 (dd, J = 8.0, 2.1 Hz, 2H, H-6 and H-6′), 2.36 (t, J = 7.6 Hz, 4H, 2 × Ph-CH_2), 1.48 (p, J = 7.6 Hz, 4H, 2 × Ph-$CH_2\underline{CH_2}$), 1.28–1.22 (m, 2H, $CH_2CH_2\underline{CH_2}CH_2CH_2$); ^{13}C NMR (150 MHz, DMSO-d6) δ 145.37 (2C), 143.48 (2C), 133.58 (2C), 119.25 (2C), 116.09 (2C), 115.83 (2C), 34.99 (2C), 31.62 (2C), 28.77; ESI-MS m/z calcd for $C_{17}H_{19}O_4$ [M - H] $^-$ 287.1, found 287.2.

*4.1.18. General procedure for the preparation of compounds 1,6-bis(3,4-dimethoxyphenyl)hexane-1,6-dione (**18a**) and 1,7-bis(3,4-dimethoxyphenyl)heptane-1,7-dione (**18b**)*

To a solution of **17** (7.20 mmol) in DCM (20 mL) at room temperature was slowly added $SOCl_2$ (5 mL). The mixture was heated at reflux for 4.5 h and the reaction solvents were removed in vacuo. The crude product was re-dissolved in DCM (5 mL), and was added dropwise to a stirring mixture of veratrole (2.00 g, 14.40 mmol) and aluminum trichloride ($AlCl_3$) (2.02 g, 15.12 mmol) in DCM (20 mL). The resulting solution was stirred at 0 °C for 5 h before pouring into ice water (50 mL). The mixture was extracted with DCM (3 × 20 mL), washed with saturated $NaHCO_3$ (20 mL) and brine. The combined organic layer was removed in vacuo to afford **18**. **18a**: white solid, yield 98%, mp: 149–151 °C; **18b**: white solid, yield 95%, mp: 156–158 °C.

*4.1.19. General procedure for the preparation of compounds 1,6-bis(3,4-dimethoxyphenyl)hexane (**19a**) and 1,7-bis(3,4-dimethoxyphenyl)heptane (**19b**)*

The title compounds **19a** and **19b** were prepared according to the procedure depicted for compound **7**. **19a**: white solid, yield 55%, mp: 66-69°C; **19b**: white solid, yield 66%, mp: 92–94 °C.

*4.1.20. General procedure for the preparation of compounds **WC3** and **WC4***

The target compound **WC3** and **WC4** were synthesized in a manner similar to the synthesis of **WA1-WA12**.

*4.1.20.1. 4,4'-(hexane-1,6-diyl)bis(benzene-1,2-diol) (**WC3**).* White solid in a yield of 80%. mp: 131–133 °C, R_f = 0.52 (DCM/MeOH = 10:1); ^{1}H NMR (400 MHz, DMSO-d_6) δ 8.66 (s, 2H, 2 × OH), 8.56 (s, 2H, 2 × OH), 6.60 (d, *J* = 7.9 Hz, 2H, H-5 and H-5′), 6.53 (d, *J* = 2.1 Hz, 2H, H-2 and H-2′), 6.39 (dd, *J* = 8.0, 2.1 Hz, 2H, H-6 and H-6′), 2.36 (t, *J* = 7.6 Hz, 4H, 2 × Ph-CH_2), 1.46 (t, *J* = 7.4 Hz, 4H, $CH_2\underline{CH_2}CH_2CH_2\underline{CH_2}CH_2$), 1.29–1.22 (m, 4H, $CH_2CH_2\underline{CH_2}\underline{CH_2}CH_2CH_2$); ^{13}C NMR (150 MHz, DMSO-d_6) δ 145.37 (2C), 143.47 (2C), 133.57 (2C), 119.25 (2C), 116.08 (2C), 115.83 (2C), 34.97 (2C), 31.66 (2C), 28.95 (2C); ESI-MS *m/z* calcd for $C_{18}H_{21}O_4$ [M - H]$^-$ 301.2, found 301.4.

*4.1.20.2. 4,4'-(Heptane-1,7-diyl)bis(benzene-1,2-diol) (**WC4**).*White solid in a yield of 62%,. mp 101–103 °C, R_f = 0.20 (DCM/MeOH = 30:1); ^{1}H NMR (600 MHz, DMSO-d_6) δ 8.67 (s, 2H, 2 × OH), 8.56 (s, 2H, 2 × OH), 6.60 (d, *J* = 7.9 Hz, 2H, H-5 and H-5′), 6.53 (d, *J* = 2.1 Hz, 2H, H-2 and H-2′), 6.39 (dd, *J* = 8.0, 2.1 Hz, 2H, H-6 and H-6′),

2.36 (t, *J* = 7.6 Hz, 4H, 2 × Ph-CH_2), 1.45 (q, *J* = 7.4 Hz, 4H, $CH_2\underline{CH_2}CH_2CH_2CH_2\underline{CH_2}CH_2$), 1.25 (ddd, *J* = 21.9, 10.9, 5.8 Hz, 6H, $CH_2CH_2\underline{CH_2}\underline{CH_2}\underline{CH_2}CH_2CH_2$); ^{13}C NMR (150 MHz, DMSO-d_6) δ 145.36 (2C), 143.46 (2C), 133.59 (2C), 119.25 (2C), 116.09 (2C), 115.83 (2C), 34.97 (2C), 31.69 (2C), 29.24, 29.10 (2C); ESI-MS *m/z* calcd for $C_{21}H_{24}O_6F_3$ $[M + CF_3COO]^-$ 429.2, found 429.5.

4.1.21. General procedure for the preparation of compounds ***21***

To a solution of corresponding aromatic acid (1.16 mmol) and 2-(1H-benzotriazol-1-yl)-*N*,*N*,*N*′,*N*′-tetramethyluronium tetrafluoroborate (TBTU) (1.16 mmol) in CH_3CN (20 mL) was slowly added 3,4-dimethoxyphenethylamine (**20**) (0.20 g, 1.10 mmol) and *N*,*N*-diisopropylethylamine (DIEA) (0.28 g, 2.20 mmol). The reaction mixture was allowed to stir for 12 h at room temperature, the solvents were removed under reduced pressure, and then water (20 mL) was added. The aqueous suspension was extracted with EtOAc (3 × 15 mL), and the resulting organic layer was washed with 1 M HCl, saturated $NaHCO_3$ and brine in turn, and was then dried over anhydrous Na_2SO_4. After removal of the solvent from the organic extracts in vacuo, the residue was purified by flash column chromatography with elution system of petroleum ether/EtOAc to afford the desired compounds **21** in yields ranging from 65-87%.

4.1.22. General procedure for the preparation of compound ***22***

Palladium on charcoal (10%, 40 mg) was added to a stirring solution of **21** containing nitro groups (0.77 mmol) in MeOH–EtOAc mixture (1:1) (20 mL) and the resulting mixture was stirred under a hydrogen balloon at room temperature for 24 h. The mixture was filtered and the residue was extracted with EtOAc (2 × 10 mL) and concentrated in vacuo to yield a crude product **22**, which was sufficiently pure to be directly used in next step.

4.1.23. General procedure for the preparation of compounds ***WD1-WD10***

The target compounds **WD1-WD10** were prepared according to the procedure depicted for compounds **WA1-WA12**.

*4.1.23.1. 4-(Tert-butyl)-N-(3,4-dihydroxyphenethyl)benzamide (**WD1**).* Yellow solid, yield 90%, mp 118–120 °C, R_f = 0.25 (DCM/MeOH = 10:1); ^{1}H NMR (400 MHz, DMSO-d_6) δ 8.74 (s, 1H, OH), 8.62 (s, 1H, OH), 8.41 (t, *J* = 5.6 Hz, 1H, NH), 7.75 (d, *J* = 8.2 Hz, 2H, H-2′ and H-6′), 7.46 (d, *J* = 8.2 Hz, 2H, H-3′ and H-5′), 6.66–6.58 (m, H-5 and H-2), 6.46 (dd, *J* = 8.0, 2.0 Hz, 1H, H-6), 3.43–3.35 (m, 2H, NH$\underline{CH_2}$), 2.64 (t, *J* = 7.5 Hz, 2H, Ph-CH_2), 1.29 (s, 9H); ^{13}C NMR (100 MHz, DMSO-d_6) δ 166.40, 154.19, 145.52, 143.97, 132.43, 130.79, 127.40 (2C), 125.43 (2C), 119.69, 116.47, 115.95, 41.70, 35.16, 35.04, 31.43 (3C); ESI-MS *m/z* calcd for $C_{19}H_{24}NO_3$ $[M + H]^+$ 314.2, found 314.4.

*4.1.23.2. N-(3,4-Dihydroxyphenethyl)-2-hydroxybenzamide (**WD2**).* White solid, yield 80%, mp 138–140 °C, R_f = 0.21 (DCM/MeOH = 10:1); ^{1}H NMR (400 MHz, DMSO-d_6) δ 12.60 (s, 1H, Ph′-OH), 8.84 (t, *J* = 5.6 Hz, 1H, NH), 8.75 (s, 1H, Ph-OH), 8.64 (s, 1H, Ph-OH), 7.82 (dd, *J* = 8.0, 1.5 Hz, 1H, H-2′), 7.42–7.33 (m, 1H, H-6′), 6.88 (t, *J* = 7.9 Hz, 2H, H-3′ and H-5′), 6.68–6.58 (m, 2H, H-5 and H-2), 6.47 (dd, *J* = 8.0, 2.0 Hz, 1H, H-6), 3.48–3.39 (m, 2H, NH$\underline{CH_2}$), 2.67 (t, *J* = 7.5 Hz, 2H, Ph-CH_2); ^{13}C NMR (100 MHz, DMSO-d_6) δ 169.24, 160.50, 145.57, 144.06, 134.05, 130.43, 128.11, 119.70, 118.98, 117.82, 116.45, 116.00, 115.72, 41.40, 34.80; ESI-MS *m/z* calcd for $C_{15}H_{16}NO_4$ $[M + H]^+$ 274.1, found 274.4.

*4.1.23.3. N-(3,4-Dihydroxyphenethyl)-4-formylbenzamide (**WD3**).* Brown solid, yield 80%, mp 120–122 °C, R_f = 0.19 (DCM/MeOH = 15:1); ^{1}H NMR (400 MHz, DMSO-d_6) δ 8.70 (s, 2H, 2 × OH), 8.61 (t, *J* = 5.6 Hz, 1H, NH), 7.77 (d, *J* = 8.5 Hz, 2H, H-2′ and H-6′), 7.67 (d, *J* = 8.4 Hz, 2H, H-3′ and H-5′), 6.67–6.56 (m, 2H, H-5 and H-2), 6.46 (dd, *J* = 8.0, 2.1 Hz, 1H, H-6), 3.36 (m, 2H, NH$\underline{CH_2}$), 2.64 (t, *J* = 7.5 Hz, 2H, Ph-CH_2); ^{13}C NMR (100 MHz, DMSO-d_6) δ 165.57, 145.53, 144.00, 134.22, 131.72 (2C), 130.67, 129.72 (2C), 125.21, 119.70, 116.47, 115.97, 41.81, 35.00; ESI-MS *m/z* calcd for $C_{15}H_{15}BrNO_3$ $[M + H]^+$ 336.0, found 336.3.

*4.1.23.4. 3,5-Diamino-N-(3,4-dihydroxyphenethyl)benzamide (**WD4**).* White solid, yield 70%, mp: 185–187 °C, R_f = 0.29 (DCM/MeOH = 10:1); ^{1}H NMR (400 MHz, DMSO-d_6) δ 8.75 (s, 1H, OH), 8.61 (s, 1H, OH), 7.98 (t, *J* = 5.7 Hz, H, NH), 6.63 (d, *J* = 7.9 Hz, 1H, H-2′), 6.59 (d, *J* = 2.1 Hz, 1H, H-6′), 6.45 (dd, *J* = 8.0, 2.1 Hz, 1H, H-5), 6.19 (d, *J* = 2.0 Hz, 2H, H-2 and h-6), 5.92 (s, 1H, H-4), 4.83 (s, 4H, 2× NH_2), 3.28 (dt, *J* = 8.5, 6.0 Hz, 2H, NH$\underline{CH_2}$), 2.58 (dd, *J* = 8.9, 6.5 Hz, 2H, Ph-CH_2); ^{13}C NMR (100 MHz, DMSO-d_6) δ 168.10, 149.39 (2C), 145.50, 143.91, 137.02, 130.88,

119.63, 116.41, 115.97, 102.50 (2C), 102.43, 41.55, 35.23; ESI-MS *m/z* calcd for $C_{15}H_{18}N_3O_3$ [M + H]$^+$ 288.1, found 288.3.

*4.1.23.5. N-(3,4-Dihydroxyphenethyl)-3,4-dihydroxybenzamide (**WD5**).* White solid, yield 87%, mp 166–168 °C, R_f = 0.21 (DCM/MeOH = 10:1); ^{1}H NMR (400 MHz, DMSO-d_6) δ 9.41 (s, 1H, OH), 9.07 (s, 1H, OH), 8.74 (s, 1H, OH), 8.62 (s, 1H, OH), 8.16 (t, *J* = 5.7 Hz, 1H, NH), 7.26 (d, *J* = 2.2 Hz, 1H, H-6′), 7.15 (dd, *J* = 8.2, 2.1 Hz, 1H, H-2′), 6.73 (d, *J* = 8.2 Hz, 1H, H-5′), 6.66–6.55 (m, 2H, H-5 and H-2), 6.45 (dd, *J* = 8.0, 2.1 Hz, 1H, H-6), 3.30 (d, *J* = 7.1 Hz, 2H, NH$\underline{CH_2}$), 2.60 (t, *J* = 7.6 Hz, 2H, Ph-CH_2); ^{13}C NMR (100 MHz, DMSO-d_6) δ 166.38, 148.62, 145.51, 145.22, 143.93, 130.89, 126.45, 119.65, 119.27, 116.43, 115.94, 115.51, 115.23, 41.67, 35.27; ESI-MS *m/z* calcd for $C_{15}H_{16}NO_5$ [M + H]$^+$ 290.1, found 290.5.

*4.1.23.6. N-(3,4-Dihydroxyphenethyl)-3,4,5-trihydroxybenzamide (**WD6**).* White solid, yield 38%, mp 198–200 °C, R_f = 0.17 (DCM/MeOH = 10:1); ^{1}H NMR (400 MHz, DMSO-d_6) δ 8.99 (s, 2H, 2 × OH), 8.74 (s, 1H, OH), 8.62 (s, 2H, OH), 8.08 (t, *J* = 5.6 Hz, 1H, NH), 6.80 (s, 2H, H-2′ and H-6′), 6.63 (d, *J* = 7.9 Hz, 1H, H-5), 6.59 (d, *J* = 2.1 Hz, 1H, H-2), 6.44 (dd, *J* = 8.0, 2.1 Hz, 1H, H-6), 3.29 (dd, *J* = 8.4, 5.9 Hz, 2H, NH$\underline{CH_2}$), 2.59 (dd, *J* = 8.8, 6.5 Hz, 2H, Ph-CH_2); ^{13}C NMR (100 MHz, DMSO-d_6) δ 166.64, 145.81 (2C), 145.50, 143.91, 136.54, 130.91, 125.53, 119.65, 116.42, 115.94, 107.11 (2C), 41.66, 35.24; ESI-MS *m/z* calcd for $C_{15}H_{16}NO_6$ [M + H]$^+$ 306.1, found 306.6.

*4.1.23.7. 4-Amino-N-(3,4-dihydroxyphenethyl)benzamide (**WD7**).* White solid, yield 72%, mp 194–195 °C, R_f = 0.23 (DCM/MeOH = 10:1); ^{1}H NMR (400 MHz, DMSO-d_6) δ 8.77 (s, 1H, OH), 8.65 (s, 1H, OH), 8.04 (t, *J* = 5.7 Hz, 1H, NH), 7.54 (d, *J* = 8.5 Hz, 2H, H-3′ and H-5′), 6.67 – 6.58 (m, 2H, H-5 and H-2′), 6.52 (d, *J* = 8.4 Hz, 2H, H-2 and H-6′), 6.45 (dd, *J* = 8.0, 2.1 Hz, 1H, H-6), 5.59 (s, 2H, NH_2), 3.31 (dd, *J* = 8.7, 5.9 Hz, 2H, NH$\underline{CH_2}$), 2.60 (dd, *J* = 8.8, 6.5 Hz, 2H, Ph-CH_2); ^{13}C NMR (100 MHz, DMSO-d_6) δ 166.53, 151.87, 145.50, 143.91, 130.97, 129.06 (2C), 121.93, 119.65, 116.44, 115.94, 113.00 (2C), 41.61, 35.44; ESI-MS *m/z* calcd for $C_{15}H_{17}N_2O_3$ [M + H]$^+$ 273.1, found 273.4.

*4.1.23.8. 2-Amino-N-(3,4-dihydroxyphenethyl)benzamide (**WD8**).* Brown solid, yield 81%, mp 168–170 °C, R_f = 0.25 (DCM/MeOH = 10:1); ^{1}H NMR (400 MHz, DMSO-d_6) δ 8.80 (s, 1H, OH), 8.68 (s, 1H, OH), 8.25 (t, *J* = 5.6 Hz, 1H, NH), 7.43 (dd, *J* = 8.0, 1.5 Hz, 1H, H-6′), 7.12 (ddd, *J* = 8.4, 7.1, 1.5 Hz, 1H, H-4′), 6.70–6.61 (m, 3H, H-5, H-3′ and H-5′), 6.52–6.44 (m, 2H, H-2 and H-6), 6.38 (s, 2H, NH_2), 3.38–3.28 (m, 2H, NH$\underline{CH_2}$), 2.70–2.58 (m, 2H, Ph-CH_2); ^{13}C NMR (100 MHz, DMSO-d_6) δ 168.54, 160.80, 145.57, 143.99, 134.05, 130.45, 128.06, 119.70, 118.98, 117.77, 116.45, 116.00, 115.74, 41.40, 34.80; ESI-MS *m/z* calcd for $C_{15}H_{17}N2O_3$ [M + H]$^+$ 273.1, found 273.3.

*4.1.23.9. N-(3,4-Dihydroxyphenethyl)-4-methylbenzamide (**WD9**).* White solid, yield 61%, mp 121–123 °C, R_f = 0.21 (DCM/MeOH = 15:1); ^{1}H NMR (400 MHz, DMSO-d_6) δ 8.75 (s, 1H, OH), 8.63 (s, 1H, OH), 8.42 (t, *J* = 5.6 Hz, 1H, NH), 7.77–7.69 (m, 2H, H-2′ and H-6′), 7.25 (d, *J* = 7.9 Hz, 2H, H-3′ and H-5′), 6.67–6.59 (m, 2H, H-5 and H-2), 6.47 (dd, *J* = 8.0, 2.0 Hz, 1H, H-6), 3.46–3.35 (m, 2H, NH$\underline{CH_2}$), 2.64 (dd, *J* = 8.7, 6.5 Hz, 2H, Ph-CH_2), 2.34 (s, 3H, CH_3); ^{13}C NMR (100 MHz, DMSO-d_6) δ 166.46, 149.08, 147.69, 141.30, 132.52, 132.35, 129.21 (2C), 127.58 (2C), 120.93, 113.03, 112.39, 41.48, 35.16, 21.37; ESI-MS *m/z* calcd for $C_{16}H_{18}NO_3$ [M + H]$^+$ 272.1, found 272.5.

*4.1.23.10. N-(3,4-Dihydroxyphenethyl)-4-(trifluoromethyl)benzamide (**WD10**).* White solid, yield 54%, mp 127–129 °C, R_f = 0.17 (DCM/MeOH = 15:1); ^{1}H NMR (400 MHz, DMSO-d_6) δ 8.80 (t, *J* = 5.6 Hz, 1H, NH), 8.77 (s, 1H, OH), 8.66 (s, 1H, OH), 8.22–8.06 (m, 2H, H-2′ and H-6′), 7.90 (d, 1H, H-3′), 7.72 (t, *J* = 7.8 Hz, 1H, H-5′), 6.62 (s, 2H, H-5 and H-2), 6.47 (dd, *J* = 8.0, 2.1 Hz, 1H, H-6), 3.41 (dt, *J* = 8.2, 6.0 Hz, 2H, NH$\underline{CH_2}$), 2.66 (dd, *J* = 8.6, 6.5 Hz, 2H, Ph-CH_2); ^{13}C NMR (150 MHz, DMSO-d_6) δ 165.01, 145.56, 144.03, 135.94, 131.71, 130.59, 130.08, 128.13, 125.38, 124.20, 123.58, 119.69, 116.45, 115.95, 41.89, 34.95; ESI-MS *m/z* calcd for $C_{16}H_{15}NF_3O_3$ [M + H]$^+$ 326.1, found 326.4.

4.2. Antibacterial evaluation

4.2.1. Antimicrobial assays

Antimicrobial assays to measure the MIC values of tested compounds were performed applying the 96-well microtitre broth dilution method as previously described [18].

4.2.2 Checkerboard titration assay

Checkerboard titration assay was used to assess the possible synergism between the antibiotics and the tested compounds as previously described [18].

4.2.3. Nile red efflux assay

The ability of tested compounds to inhibit substrate transport mediated by AcrB was evaluated by determining the reduction in Nile Red efflux as previously described [18].

4.2.4. Nitrocefin uptake assay

The ability of tested compounds to permeabilize outer membrane of *E. coli* BW25513 was assessed by using nitrocefin uptake assay as described previously [18, 51].

4.2.5. Measurement of the electrochemical gradient over the inner membrane

The influence of tested compounds on the membrane potential ($\Delta\psi$) across the inner-membrane of *E. coli* BW25513 was investigated by determining fluorescence intensity of the fluorescent probe $DiOC_2$ (3) as previously described [18, 51].

Conflicts of interest

The authors declare that this study was carried out only with public funding. There is no funding or no agreement with commercial for profit firms.

Acknowledgments

This research was supported financially by the National Natural Science Foundation of China (81973179 and 81673284), the National Health and Medical Research Council of Australia (GN1147538), Key research and development project of Shandong Province (2017CXGC1401) and Major Project of Research and development of Shandong Province (2019GSF108051). RA is the recipient of a PhD scholarship from the Government of Saudi Arabia.

References

[1] O. Nolte, Antimicrobial resistance in the 21st century: a multifaceted challenge, Protein Peptide Lett. 21 (2014) 330-335.

[2] H.W. Boucher, G.H. Talbot, J.S. Bradley, J.E. Edwards, D. Gilbert, L.B. Rice, M. Scheld, B. Spellberg, J. Bartlett, Bad bugs, no drugs: no ESKAPE! An update from the Infectious Diseases Society of America, Clin. Infect. Dis. 48 (2009) 1-12.

[3] J. Cole, Antimicrobial resistance--a 'rising tide' of national (and international) risk, J. Hosp. Infect. 92 (2016) 3-4.

[4] T.J. Opperman, S.M. Kwasny, H.S. Kim, S.T. Nguyen, C. Houseweart, S. D'Souza, G.C. Walker, N.P. Peet, H. Nikaido, T.L. Bowlin, Characterization of a novel pyranopyridine inhibitor of the AcrAB efflux pump of *Escherichia coli*, Antimicrob. Agents Chemother. 58 (2014) 722-733.

[5] F. WHO, OIE (2018) Monitoring global progress on addressing antimicrobial resistance: analysis report of the second round of results of AMR country self-assessment survey 2018, World Health Organization, Food and Agriculture Organization of the United Nations and World Organisation for Animal Health (OIE), Geneva.

[6] C.A. Arias, B.E. Murray, Antibiotic-resistant bugs in the 21st century--a clinical super-challenge, N. Engl. J. Med. 360 (2009) 439-443.

[7] R.P. Rennie, Current and future challenges in the development of antimicrobial agents, Handb. Exp. Pharmacol. 211 (2012) 45-65.

[8] S. Harbarth, G. Kahlmeter, J. Kluytmans, M. Mendelson, C. Town, S. Africa, C. Pulcini, N. Singh, U. Theuretzbacher, C. Food, Global priority list of antibiotic-resistant bacteria to guide research, discovery, and development of new antibiotics, in, WHO, 2017.

[9] K. Bush, P. Courvalin, G. Dantas, J. Davies, B. Eisenstein, P. Huovinen, G.A. Jacoby, R. Kishony, B.N.

Kreiswirth, E. Kutter, S.A. Lerner, S. Levy, K. Lewis, O. Lomovskaya, J.H. Miller, S. Mobashery, L.J. Piddock, S. Projan, C.M. Thomas, A. Tomasz, P.M. Tulkens, T.R. Walsh, J.D. Watson, J. Witkowski, W. Witte, G. Wright, P. Yeh, H.I. Zgurskaya, Tackling antibiotic resistance, Nat. Rev. Microbiol. 9 (2011) 894-896.

[10] M. Zwama, S. Yamasaki, R. Nakashima, K. Sakurai, Multiple entry pathways within the efflux transporter AcrB contribute to multidrug recognition, Nat. Commun. 9 (2018) 124.

[11] H. Venter, R. Mowla, T. Ohene-Agyei, S. Ma, RND-type drug efflux pumps from Gram-negative bacteria: molecular mechanism and inhibition, Front. Microbiol. 6 (2015) 377.

[12] X.Z. Li, P. Plesiat, H. Nikaido, The challenge of efflux-mediated antibiotic resistance in Gram-negative bacteria, Clin. Microbiol. Rev. 28 (2015) 337-418.

[13] M.H. Nicolas-Chanoine, N. Mayer, K. Guyot, E. Dumont, J.M. Pages, Interplay between membrane permeability and enzymatic barrier leads to antibiotic-dependent resistance in *Klebsiella pneumoniae*, Front. Microbiol. 9 (2018) 1422.

[14] H.I. Zgurskaya, C.A. Lopez, S. Gnanakaran, Permeability barrier of Gram-negative cell envelopes and approaches To bypass it, ACS Infect Dis. 1 (2015) 512-522.

[15] J.R. Aires, T. Kohler, H. Nikaido, P. Plesiat, Involvement of an active efflux system in the natural resistance of *Pseudomonas aeruginosa* to aminoglycosides, Antimicrob. Agents Chemother. 43 (1999) 2624-2628.

[16] X. Yang, S. Goswami, B.K. Gorityala, R. Domalaon, Y. Lyu, A. Kumar, G.G. Zhanel, F. Schweizer, A tobramycin vector enhances synergy and efficacy of efflux pump inhibitors against multidrug-resistant Gram-negative bacteria, J. Med. Chem. 60 (2017) 3913-3932.

[17] K.M. Haynes, N. Abdali, V. Jhawar, H.I. Zgurskaya, J.M. Parks, Identification and structure-Activity relationships of novel compounds that potentiate the activities of antibiotics in *Escherichia coli*, J. Med. Chem. 60 (2017) 6205-6219.

[18] Y. Wang, R. Mowla, S. Ji, L. Guo, M.A. De Barros Lopes, C. Jin, D. Song, S. Ma, H. Venter, Design, synthesis and biological activity evaluation of novel 4-subtituted 2-naphthamide derivatives as AcrB inhibitors, Eur. J. Med. Chem. 143 (2018) 699-709.

[19] M. Arzanlou, W.C. Chai, H. Venter, Intrinsic, adaptive and acquired antimicrobial resistance in Gram-negative bacteria, Essays Biochem. 61 (2017) 49-59.

[20] S.H. Ardehali, T. Azimi, F. Fallah, M. Owrang, N. Aghamohammadi, L. Azimi, Role of efflux pumps in reduced susceptibility to tigecycline in Acinetobacter baumannii, New Microbes New infect. 30 (2019) 100547.

[21] J.W. Handing, S.A. Ragland, U.V. Bharathan, A.K. Criss, The MtrCDE efflux pump contributes to survival of *Neisseria gonorrhoeae* from human neutrophils and their antimicrobial components, Front. Microbiol. 9 (2018) 2688.

[22] H. Nikaido, H.I. Zgurskaya, AcrAB and related multidrug efflux pumps of *Escherichia coli*, J. Mol. Microbiol. Biotechnol. 3 (2001) 215-218.

[23] Y. Wang, H. Venter, S. Ma, Efflux Pump Inhibitors: A novel approach to combat efflux-mediated drug resistance in bacteria, Curr. Drug Targets 17 (2016) 702-719.

[24] A. Welch, C.U. Awah, S. Jing, H.W. van Veen, H. Venter, Promiscuous partnering and independent activity of MexB, the multidrug transporter protein from *Pseudomonas aeruginosa*, Biochem. J. 430 (2010) 355-364.

[25] L. Daury, F. Orange, J.C. Taveau, A. Verchere, L. Monlezun, C. Gounou, R.K. Marreddy, M. Picard, I. Broutin, K.M. Pos, O. Lambert, Tripartite assembly of RND multidrug efflux pumps, Nat. commun. 7 (2016) 10731.

[26] D. Du, Z. Wang, N.R. James, J.E. Voss, E. Klimont, T. Ohene-Agyei, H. Venter, W. Chiu, B.F. Luisi, Structure of the AcrAB-TolC multidrug efflux pump, Nature 509 (2014) 512-515.

[27] G. Krishnamoorthy, E.B. Tikhonova, G. Dhamdhere, H.I. Zgurskaya, On the role of TolC in multidrug efflux: the function and assembly of AcrAB-TolC tolerate significant depletion of intracellular TolC protein, Mol. Microbiol. 87 (2013) 982-997.

[28] S. Murakami, R. Nakashima, E. Yamashita, T. Matsumoto, A. Yamaguchi, Crystal structures of a multidrug

transporter reveal a functionally rotating mechanism, Nature 443 (2006) 173-179.

[29] M.A. Seeger, A. Schiefner, T. Eicher, F. Verrey, K. Diederichs, K.M. Pos, Structural asymmetry of AcrB trimer suggests a peristaltic pump mechanism, Science 313 (2006) 1295-1298.

[30] T. Eicher, L. Brandstatter, K.M. Pos, Structural and functional aspects of the multidrug efflux pump AcrB, Biol. Chem. 390 (2009) 693-699.

[31] K.M. Pos, Drug transport mechanism of the AcrB efflux pump, Biochim. Biophys. Acta 1794 (2009) 782-793.

[32] T. Ohene-Agyei, J.D. Lea, H. Venter, Mutations in MexB that affect the efflux of antibiotics with cytoplasmic targets, FEMS Microbiol. Lett. 333 (2012) 20-27.

[33] P. Ruggerone, S. Murakami, K.M. Pos, A.V. Vargiu, RND efflux pumps: structural information translated into function and inhibition mechanisms, Curr. Top. Med. Chem. 13 (2013) 3079-3100.

[34] V.K. Ramaswamy, A.V. Vargiu, G. Malloci, J. Dreier, P. Ruggerone, Molecular determinants of the promiscuity of MexB and MexY multidrug transporters of *Pseudomonas aeruginosa*, Front.Microbiol. 9 (2018) 1144.

[35] J.M. Blair, H.E. Smith, V. Ricci, A.J. Lawler, L.J. Thompson, L.J. Piddock, Expression of homologous RND efflux pump genes is dependent upon AcrB expression: implications for efflux and virulence inhibitor design, J. Antimicrob. Chemother. 70 (2015) 424-431.

[36] H. Venter, Reversing resistance to counter antimicrobial resistance in the World Health Organisation's critical priority of most dangerous pathogens, Biosci. Rep. 39 (2019).

[37] V.K. Ramaswamy, P. Cacciotto, G. Malloci, A.V. Vargiu, P. Ruggerone, Computational modelling of efflux pumps and their inhibitors, Essays Biochem. 61 (2017) 141-156.

[38]J.M. Pages, M. Masi, J. Barbe, Inhibitors of efflux pumps in Gram-negative bacteria, Trends Mol. Med. 11 (2005) 382-389.

[39] R. Nakashima, K. Sakurai, S. Yamasaki, K. Hayashi, C. Nagata, K. Hoshino, Y. Onodera, K. Nishino, A. Yamaguchi, Structural basis for the inhibition of bacterial multidrug exporters, Nature 500 (2013) 102-106.

[40] V. Sousa, A. Luis, M. Oleastro, F. Domingues, S. Ferreira, Polyphenols as resistance modulators in *Arcobacter butzleri*, Folia Microbiol. (Praha) 64 (2019) 547-554.

[41] C.R. Sturge, C.F. Felder-Scott, R. Pifer, C. Pybus, R. Jain, B.L. Geller, D.E. Greenberg, AcrAB-TolC inhibition by peptide-conjugated phosphorodiamidate morpholino oligomers restores antibiotic activity in Vitro and in Vivo, ACS Infec. Dis. (2019).

[42] A. Tariq, M. Sana, A. Shaheen, F. Ismat, S. Mahboob, W. Rauf, O. Mirza, M. Iqbal, M. Rahman, Restraining the multidrug efflux transporter STY4874 of Salmonella Typhi by reserpine and plant extracts, Lett. Appl. Microbiol. (2019).

[43] Y. Wang, R. Mowla, L. Guo, A.D. Ogunniyi, T. Rahman, M.A. De Barros Lopes, S. Ma, H. Venter, Evaluation of a series of 2-napthamide derivatives as inhibitors of the drug efflux pump AcrB for the reversal of antimicrobial resistance, Bioorg. Med. Chem. Lett. 27 (2017) 733-739.

[44] R. Nakashima, K. Sakurai, S. Yamasaki, K. Nishino, A. Yamaguchi, Structures of the multidrug exporter AcrB reveal a proximal multisite drug-binding pocket, Nature 480 (2011) 565-569.

[45]H. Sjuts, A.V. Vargiu, S.M. Kwasny, S.T. Nguyen, H.S. Kim, X. Ding, A.R. Ornik, P. Ruggerone, T.L. Bowlin, H. Nikaido, K.M. Pos, T.J. Opperman, Molecular basis for inhibition of AcrB multidrug efflux pump by novel and powerful pyranopyridine derivatives, Proc. Natl. Acad. Sci. U. S. A. 113 (2016) 3509-3514.

[46] A. Yamaguchi, R. Nakashima, K. Sakurai, Structural basis of RND-type multidrug exporters, Front. Microbiol. 6 (2015) 327.

[47] T. Eicher, H.J. Cha, M.A. Seeger, L. Brandstatter, J. El-Delik, J.A. Bohnert, W.V. Kern, F. Verrey, M.G. Grutter, K. Diederichs, K.M. Pos, Transport of drugs by the multidrug transporter AcrB involves an access and a deep binding pocket that are separated by a switch-loop, Proc. Natl. Acad. Sci. U. S. A. 109 (2012) 5687-5692.

[48] J. Dreier, P. Ruggerone, Interaction of antibacterial compounds with RND efflux pumps in *Pseudomonas aeruginosa*, Front. Microbiol. 6 (2015) 660.

[49] I. Malvacio, R. Buonfiglio, N. D'Atanasio, G. Serra, A. Bosin, F.P. Di Giorgio, P. Ruggerone, R. Ombrato, A.V. Vargiu, Molecular basis for the different interactions of congeneric substrates with the polyspecific transporter AcrB, Biochim. Biophys. Acta Biomembr. 1861 (2019) 1397-1408.

[50] T. Ohene-Agyei, R. Mowla, T. Rahman, H. Venter, Phytochemicals increase the antibacterial activity of antibiotics by acting on a drug efflux pump, MicrobiologyOpen 3 (2014) 885-896.

[51] O. Lomovskaya, M.S. Warren, A. Lee, J. Galazzo, R. Fronko, M. Lee, J. Blais, D. Cho, S. Chamberland, T. Renau, R. Leger, S. Hecker, W. Watkins, K. Hoshino, H. Ishida, V.J. Lee, Identification and characterization of inhibitors of multidrug resistance efflux pumps in *Pseudomonas aeruginosa*: novel agents for combination therapy, Antimicrob. Agents Chemother. 45 (2001) 105-116.

[52] J.A. Bohnert, B. Karamian, H. Nikaido, Optimized Nile Red efflux assay of AcrAB-TolC multidrug efflux system shows competition between substrates, Antimicrob. Agents Chemother. 54 (2010) 3770-3775.

[53] T.J. Opperman, S.T. Nguyen, Recent advances toward a molecular mechanism of efflux pump inhibition, Front. Microbiol. 6 (2015) 421.

[54] J.A. Bohnert, S. Schuster, W.V. Kern, T. Karcz, A. Olejarz, A. Kaczor, J. Handzlik, K. Kiec-Kononowicz, Novel piperazine arylideneimidazolones inhibit the AcrAB-TolC pump in *Escherichia coli* and simultaneously act as fluorescent membrane probes in a combined real-time influx and efflux Assay, Antimicrob. Agents Chemother. 60 (2016) 1974-1983.

[55] H. Venter, R.A. Shilling, S. Velamakanni, L. Balakrishnan, H.W. Van Veen, An ABC transporter with a secondary-active multidrug translocator domain, Nature 426 (2003) 866-870.

Fig. 1. Molecular docking of NDGA [50]. (a) Chemical structure of NDGA; (b) Overlay of NDGA (yellow) on the crystal structure of AcrB with minocycline (red); (c) The interaction of NDGA with the amino acids of AcrB.

Fig. 2. Inhibition of AcrB-mediated Nile Red efflux. Wild-type resistant cells with active pump (solid black line), ΔAcrB drug-sensitive cells (grey line) or wild-type cells in the presence of the compounds tested (dotted lines) were preloaded with Nile Red before the start of fluorescence measurements. Efflux was triggered at 100 sec by the addition of 0.2% glucose (indicated by arrow). Representative fluorescent traces are shown for triplicate experiments with different batches of cells.

Fig. 3. The effect of compounds tested on outer membrane permeability. *E. coli* were treated with 10 μM CCCP to inhibit the efflux of nitrocefin. Nitrocefin was added to the cells that received no compound (blue circles), cells treated with the outer membrane permeabilizer polymyxin B (red squares) or the test compounds (red triangles). Nitrocefin hydrolysis by the periplasmic β-lactamase was observed as an increase in absorbance at 490 nm. Representative traces are shown from duplicate experiments performed on different days.

Fig. 4. The effect of the selected compounds tested on pmf of inner membrane. Bacterial suspensions were either left untreated (solid blue line) or exposed to 8-256 μg/mL test compounds (broken red line) for 10 min after which the potentiometric probe, $DiOC_2(3)$ was added and the fluorescence monitored until it plateaued. Cells were then re-energized with 0.5% glucose and the establishment of a membrane potential (inside negative) was measured as an increase in fluorescence until it plateaued. The membrane potential was then disrupted by the addition of the proton ionophore CCCP (observed as a sharp drop in fluorescence intensity).

Fig. 5. *In silico* docking studies. The molecular interactions of AcrB with (a) **WA7** and (b) **WD6**.

Scheme 1 Reagents and conditions: a) $CH_2(COOH)_2$, piperidine, pyridine, reflux, 90%; b) $LiAlH_4$, THF, 83%; c) PPh_3, CBr_4, 87%; d) PPh_3, toluene, reflux, 62%; e) ArCHO, n-butyllithium, THF, 45-82%; f) Pd/C, H_2, rt; g) BBr_3, 37-76% in two steps for **WA1**-**WA12**, 34-86% in two steps for **WB1**-**WB11**.

Scheme 2 Reagents and conditions: a) NaOH, EtOH, reflux, 90%; b) Pd/C, H_2, MeOH, rt, 97%; c) $NaBH_4$, MeOH, rt, 96%; d) H_2SO_4, 1,4-dioxane, 68%; e) Pd/C, H_2, MeOH, rt, 82%; f) BBr_3, 71%.

Scheme 3 Reagents and conditions: a) acetone, NaOH, EtOH, 87%; b) Pd/C, H_2, MeOH/AcOEt, rt, 95%; c) $N_2H_4 \cdot H_2O$, KOH, glycol, 96%; d) BBr_3, 47%.

Scheme 4 Reagents and conditions: a) $SOCl_2$, 1,2-dimethoxybenzene, then $AlCl_3$, 95-98%; b) Pd/C, H_2, MeOH/EtOAc, rt, 55-66%; c) BBr_3, 62-80%.

Scheme 5 Reagents and conditions: a) TBTU, DIEA, CH_3CN, 65-87%; b) Pd/C, H_2, MeOH/EtOAc, rt; c) BBr_3, 38-90% for **WD1**-**WD3**, **WD5**, **WD6**, **WD9** and **WD10**, 70-81% for **WD4**, **WD7** and **WD8**.

Table 1. The synergistic effect of NDGA analogues (Series **WA-WC**) with different antibacterials against wild-type drug-resistant strain *E. coli* BW25113 expressing AcrB that is indicated as (+)AcrB.

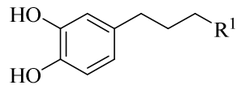

Compd.	R^1	Conc. (μg/mL)	MIC (μg/mL) CAM	ERY	TPP	LEV	RIF	Compd.	R^1	Conc. (μg/mL)	MIC (μg/mL) CAM	ERY	TPP	LEV	RIF
WA5	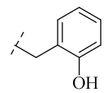	16	8	64	512	0.06	16	WB11	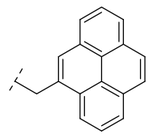	16	8	64	512	0.06	16
		32	4	64	512	0.06	16			32	8	64	512	0.06	16
		64	4	64	512	0.06	16			64	8	32	512	0.06	16
		128	4	64	512	0.06	16			128	4	32	256	0.06	16
		256	4	32	512	0.06	16			256	4	32	256	0.06	16
WA6	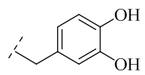	16	8	64	1024	0.06	16	WC1	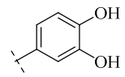	16	8	64	1024	0.06	16
		32	8	64	1024	0.06	16			32	8	64	1024	0.06	16
		64	8	64	512	0.06	16			64	8	32	512	0.06	16
		128	8	32	512	0.06	16			128	8	32	512	0.06	16
		256	4	32	512	0.06	16			256	8	32	512	0.06	16
WA7	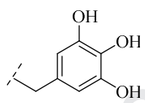	16	8	64	512	0.06	16	WC2	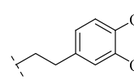	16	8	64	1024	0.06	16
		32	8	64	512	0.06	16			32	8	64	1024	0.06	16
		64	8	32	512	0.06	16			64	8	64	1024	0.06	16
		128	8	32	256	0.06	16			128	8	64	512	0.06	16
		256	1	32	256	0.06	16			256	8	64	32	0.06	16
WA9	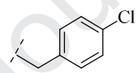	16	16	64	1024	0.06	16	WC3	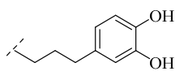	16	8	64	512	0.06	16
		32	16	64	1024	0.06	16			32	8	64	512	0.06	16
		64	16	64	512	0.06	16			64	8	64	512	0.06	16
		128	16	64	512	0.06	16			128	8	64	512	0.06	16
		256	16	64	512	0.06	16			256	8	64	512	0.06	16
WA10	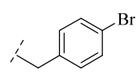	16	8	64	1024	0.06	16	WC4	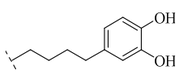	16	8	64	1024	0.06	16
		32	8	64	1024	0.06	16			32	8	64	512	0.06	16
		64	8	64	512	0.06	16			64	8	64	512	0.06	16
		128	8	64	512	0.06	16			128	8	64	512	0.06	16
		256	8	64	512	0.06	16			256	8	64	512	0.06	16
NDGA		32	8	64	1024	0.06	16	NONE	(+)AcrB	0	8	64	1024	0.06	16
		64	8	64	1024	0.03	16	NONE	(-)AcrB	0	2	4	32	0.004	16
		128	4	64	128	0.03	16								
		256	2	32	64	0.03	16								

CAM = Chloramphenicol; ERY = Erythromycin; TPP = Tetraphenylphosphonium; LEV = levofloxacin; RIF = Rifampicin

Table 2. The synergistic effect of NDGA derivatives (Series **WD**) with different antibacterials against wild-type drug-resistant strain *E. coli* BW25113 expressing AcrB that is indicated as (+)AcrB.

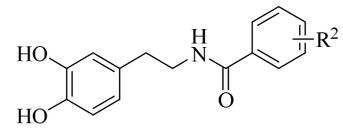

Compd.	R^2	Conc. (μg/mL)	MIC (μg/mL)					Compd.	R^2	Conc. (μg/mL)	MIC (μg/mL)					
			CAM	ERY	TPP	LEV	RIF				CAM	ERY	TPP	LEV	RIF
WD2	2-OH	8	8	64	1024	0.06	16	WD7	4-NH_2	8	8	64	1024	0.06	16
		16	8	64	1024	0.06	16			16	4	64	1024	0.06	16
		32	8	64	1024	0.03	16			32	4	32	1024	0.06	16
		64	8	64	512	0.03	16			64	4	32	1024	0.06	16
		128	4	64	512	0.03	16			128	2	16	512	0.06	16
WD3	4-Br	8	8	64	1024	0.06	16	WD8	2-NH_2	8	8	64	1024	0.06	16
		16	8	64	1024	0.06	16			16	8	64	1024	0.06	16
		32	8	64	1024	0.06	16			32	8	64	1024	0.06	16
		64	8	64	1024	0.06	16			64	4	64	1024	0.06	16
		128	8	32	1024	0.06	16			128	4	32	512	0.06	16
WD4	3,5-di-NH_2	8	8	64	512	0.06	16	WD9	4-CH_3	8	8	64	1024	0.06	16
		16	8	64	512	0.06	16			16	8	32	1024	0.06	16
		32	8	32	512	0.06	16			32	8	16	1024	0.06	16
		64	8	32	512	0.06	16			64	N/D	N/D	N/D	N/D	16
		128	8	32	512	0.06	16			128	N/D	N/D	N/D	N/D	16
WD5	3,4-di-OH	8	8	64	1024	0.06	16	WD10	4-CF_3	8	8	64	1024	0.06	16
		16	4	64	1024	0.06	16			16	8	64	1024	0.06	16
		32	4	32	512	0.06	16			32	8	64	1024	0.06	16
		64	2	32	512	0.06	16			64	8	64	1024	0.06	16
		128	2	32	512	0.06	16			128	8	64	1024	0.03	16
WD6	3,4,5-tri-OH	8	4	32	1024	0.06	16	NDGA		32	8	64	1024	0.06	16
		16	4	32	1024	0.06	16			64	8	64	1024	0.03	16
		32	4	32	512	0.03	16			128	4	64	128	0.03	16
		64	4	16	512	0.03	16			256	2	32	64	0.03	16
		128	2	16	256	0.03	16	NONE	(+)AcrB	0	8	64	1024	0.06	16
								NONE	(-)AcrB	0	2	4	32	0.004	16

CAM = Chloramphenicol; ERY = Erythromycin; TPP = Tetraphenylphosphonium; LEV = levofloxacin; RIF = Rifampicin

Fig. 1

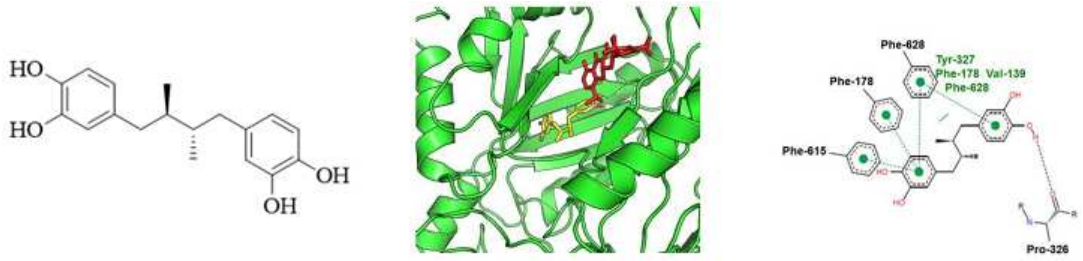

a b c

Fig. 2

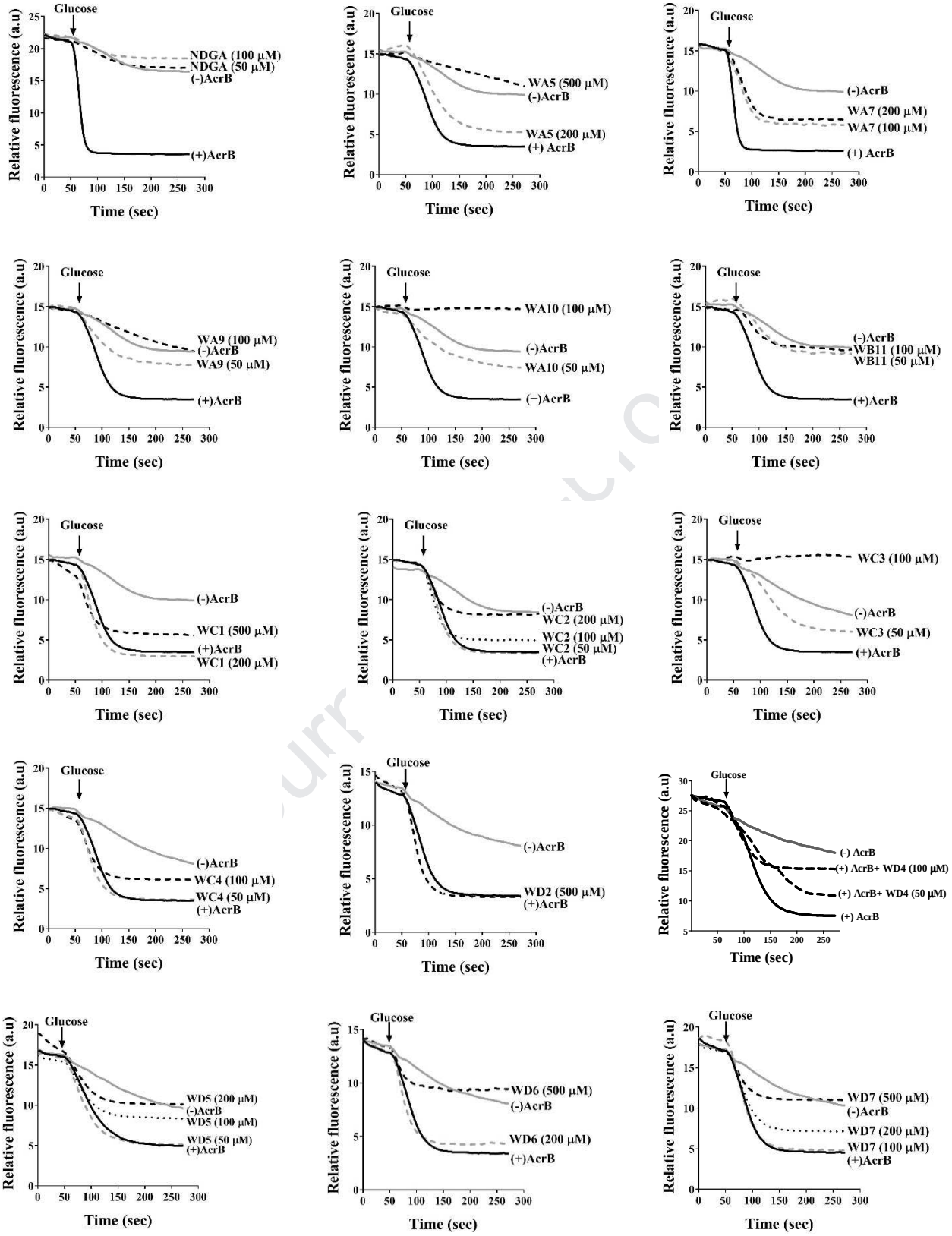
Glucose
Relative fluorescence (a.u)
Time (sec)
NDGA (100 μM)
NDGA (50 μM)
(-)AcrB
(+)AcrB
WA5 (500 μM)
WA5 (200 μM)
WA7 (200 μM)
WA7 (100 μM)
WA9 (100 μM)
WA9 (50 μM)
WA10 (100 μM)
WA10 (50 μM)
WB11 (100 μM)
WB11 (50 μM)
WC1 (500 μM)
WC1 (200 μM)
WC2 (200 μM)
WC2 (100 μM)
WC2 (50 μM)
WC3 (100 μM)
WC3 (50 μM)
WC4 (100 μM)
WC4 (50 μM)
WD2 (500 μM)
(-) AcrB
(+) AcrB+ WD4 (100 μM)
(+) AcrB+ WD4 (50 μM)
(+) AcrB
WD5 (200 μM)
WD5 (100 μM)
WD5 (50 μM)
WD6 (500 μM)
WD6 (200 μM)
WD7 (500 μM)
WD7 (200 μM)
WD7 (100 μM)

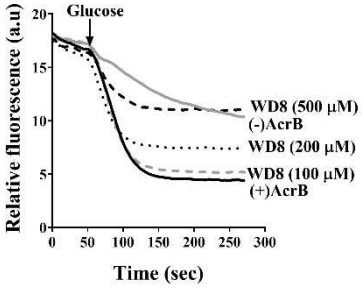

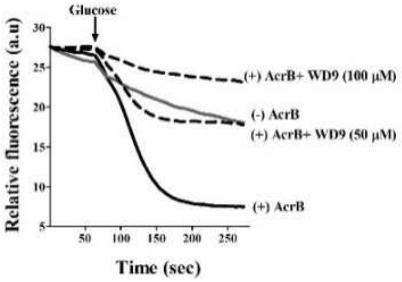

Fig. 3

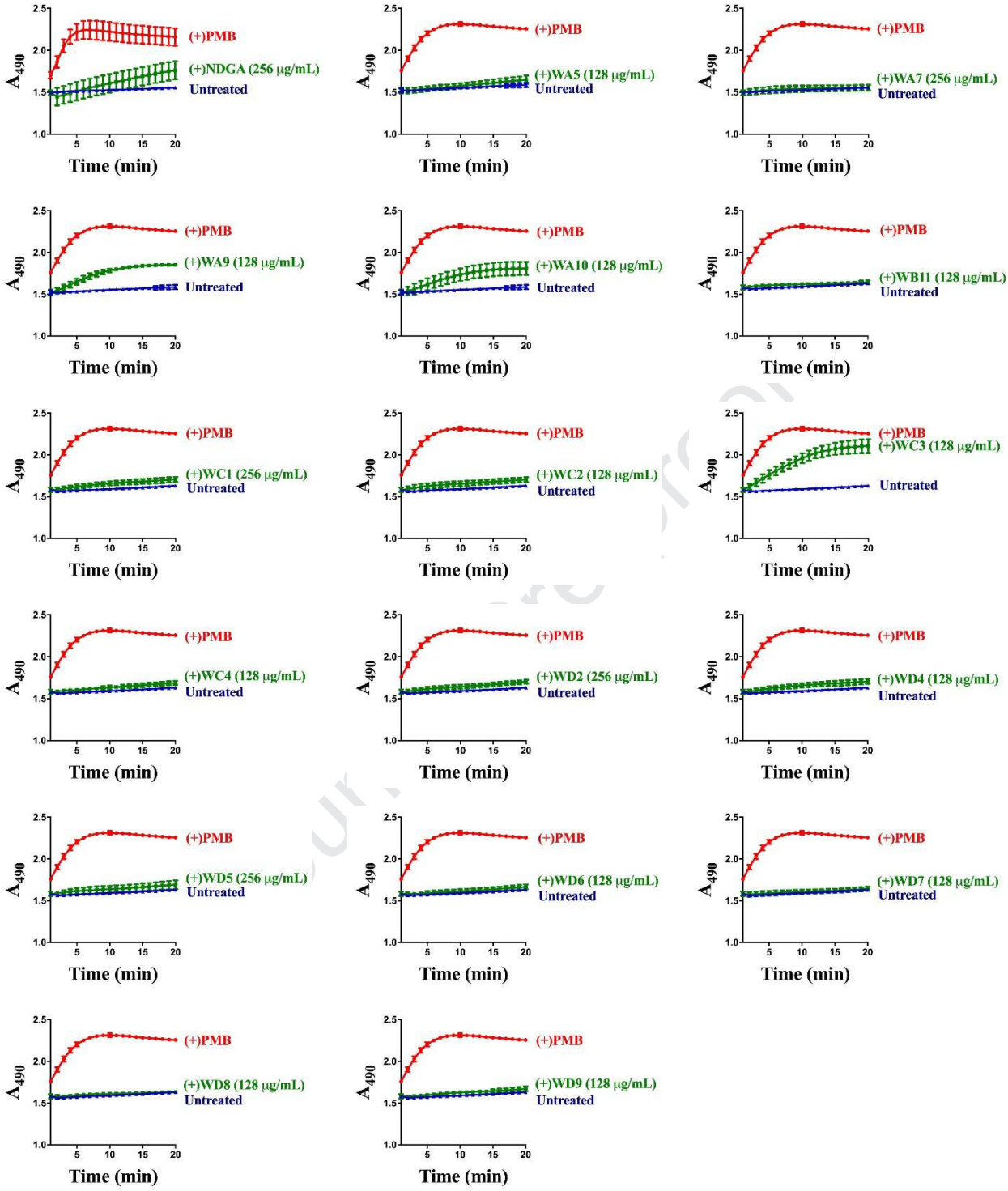
A490
Time (min)
(+)PMB
(+)NDGA (256 μg/mL)
Untreated
(+)WA5 (128 μg/mL)
(+)WA7 (256 μg/mL)
(+)WA9 (128 μg/mL)
(+)WA10 (128 μg/mL)
(+)WB11 (128 μg/mL)
(+)WC1 (256 μg/mL)
(+)WC2 (128 μg/mL)
(+)WC3 (128 μg/mL)
(+)WC4 (128 μg/mL)
(+)WD2 (256 μg/mL)
(+)WD4 (128 μg/mL)
(+)WD5 (256 μg/mL)
(+)WD6 (128 μg/mL)
(+)WD7 (128 μg/mL)
(+)WD8 (128 μg/mL)
(+)WD9 (128 μg/mL)

Fig. 4

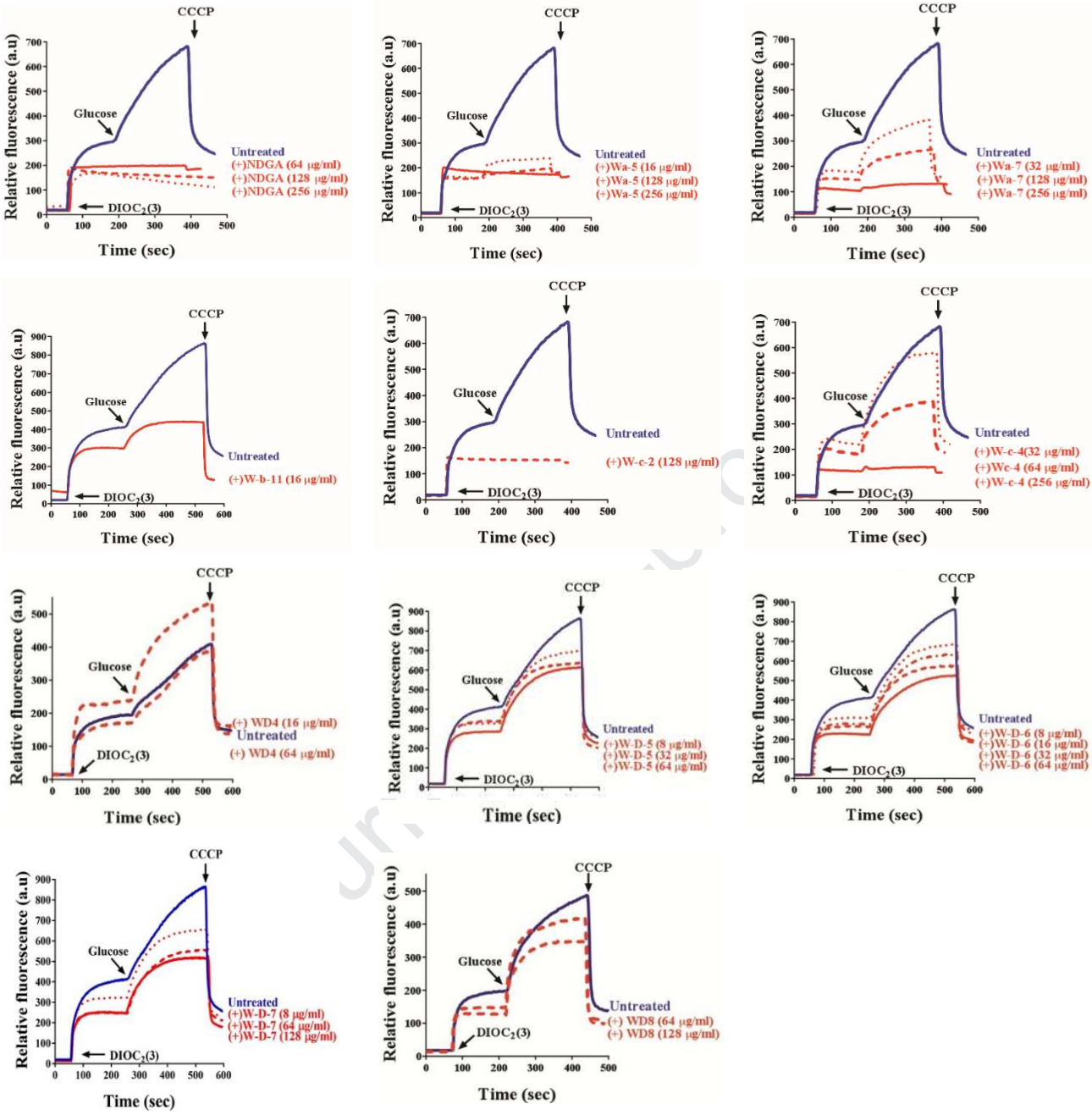
CCCP
Glucose
DIOC2(3)
Relative fluorescence (a.u)
Time (sec)
Untreated
(+)NDGA (64 μg/ml)
(+)NDGA (128 μg/ml)
(+)NDGA (256 μg/ml)
(+)Wa-5 (16 μg/ml)
(+)Wa-5 (128 μg/ml)
(+)Wa-5 (256 μg/ml)
(+)Wa-7 (32 μg/ml)
(+)Wa-7 (128 μg/ml)
(+)Wa-7 (256 μg/ml)
(+)W-b-11 (16 μg/ml)
(+)W-c-2 (128 μg/ml)
(+)W-c-4(32 μg/ml)
(+)Wc-4 (64 μg/ml)
(+)W-c-4 (256 μg/ml)
(+) WD4 (16 μg/ml)
(+) WD4 (64 μg/ml)
(+)W-D-5 (8 μg/ml)
(+)W-D-5 (32 μg/ml)
(+)W-D-5 (64 μg/ml)
(+)W-D-6 (8 μg/ml)
(+)W-D-6 (16 μg/ml)
(+)W-D-6 (32 μg/ml)
(+)W-D-6 (64 μg/ml)
(+)W-D-7 (8 μg/ml)
(+)W-D-7 (64 μg/ml)
(+)W-D-7 (128 μg/ml)
(+) WD8 (64 μg/ml)
(+) WD8 (128 μg/ml)

Fig. 5

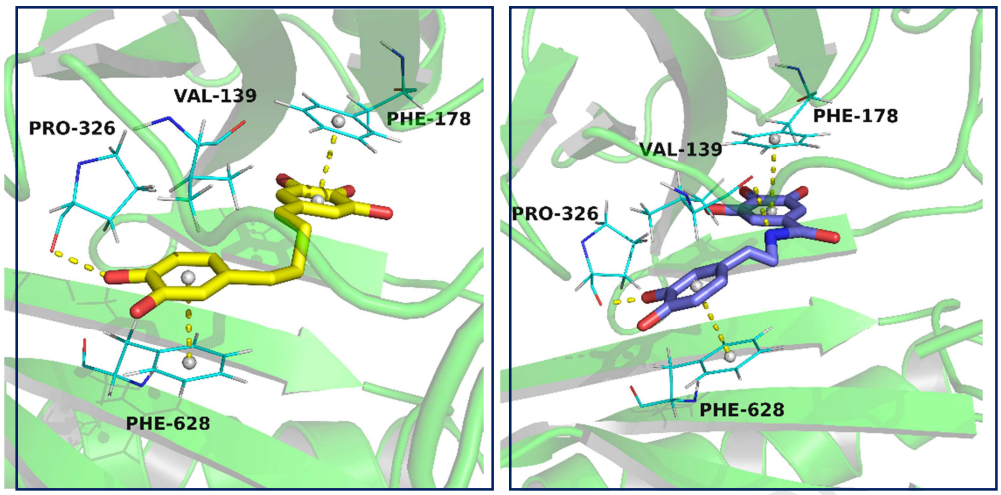

a b

Scheme 1

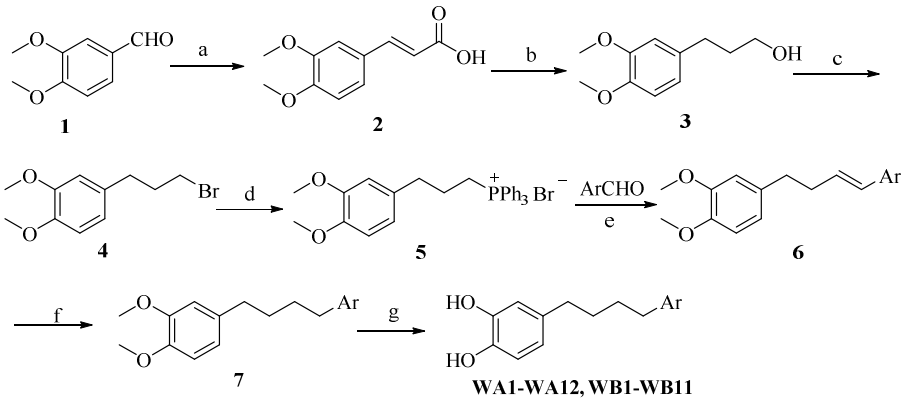

WA1 Ar = phenyl
WA2 Ar = 4-methylphenyl
WA3 Ar = 4-isopropylphenyl
WA4 Ar = 4-hydroxyphenyl
WA5 Ar = 2-hydroxyphenyl
WA6 Ar = 3,4-dihydroxyphenyl
WA7 Ar = 3,4,5-trihydroxyphenyl
WA8 Ar = 4-fluorophenyl
WA9 Ar = 4-chlorophenyl
WA10 Ar = 4-bromophenyl
WA11 Ar = 4-tert-butylphenyl
WA12 Ar = 4-aminophenyl
WB1 Ar = pyridin-2-yl
WB2 Ar = furan-2-yl
WB3 Ar = pyridin-4-yl
WB4 Ar = 1,1'-biphenyl-4-yl
WB5 Ar = 4,4'-diphenyl
WB6 Ar = naphthalen-1-yl
WB7 Ar = 6-hydroxynaphthalen-2-yl
WB8 Ar = 1-methyl-1*H*-indol-3-yl
WB9 Ar= 1-isopentyl-1*H*-indol-3-yl
WB10 Ar = anthracen-9-yl
WB11 Ar = pyren-4-yl

Scheme 2

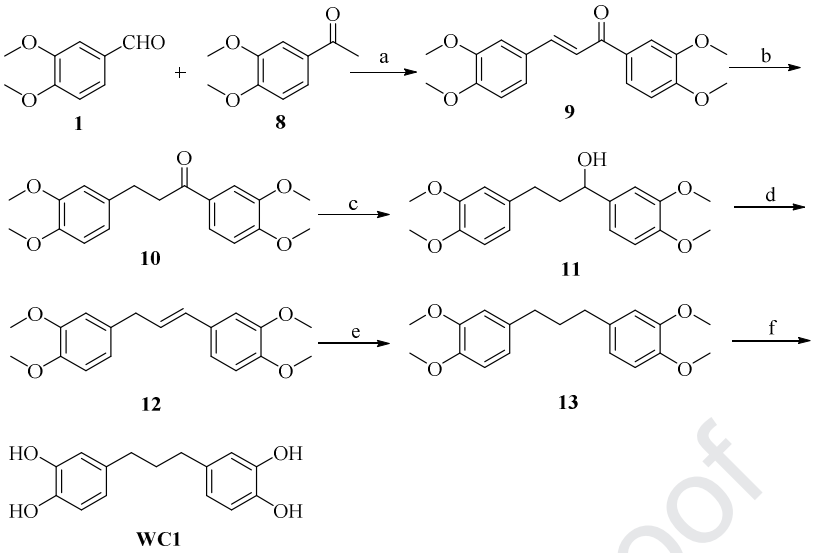

1 **8** **9** **10** **11** **12** **13** **WC1**

Scheme 3

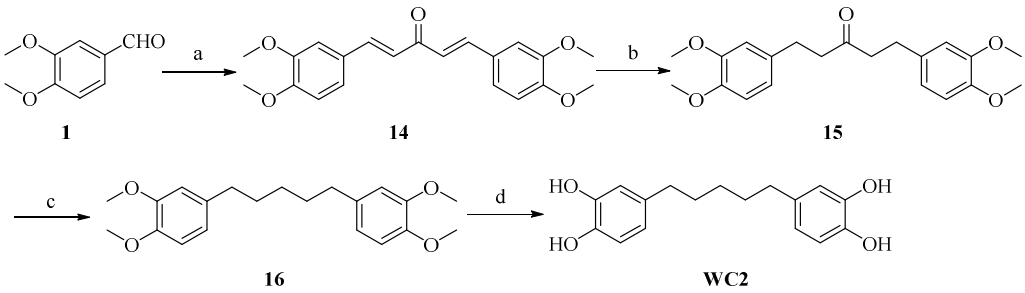

Scheme 4

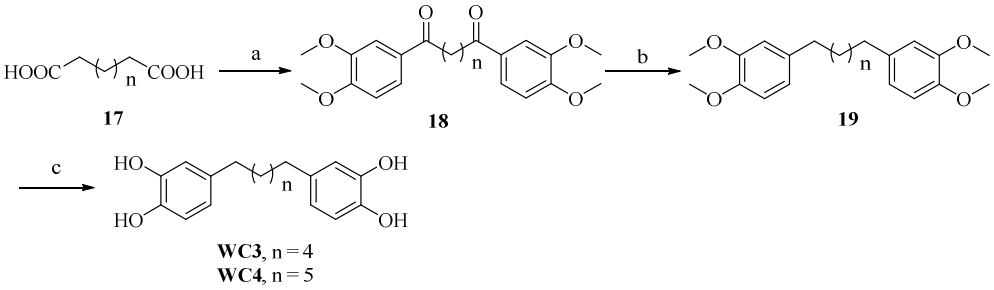

Scheme 5

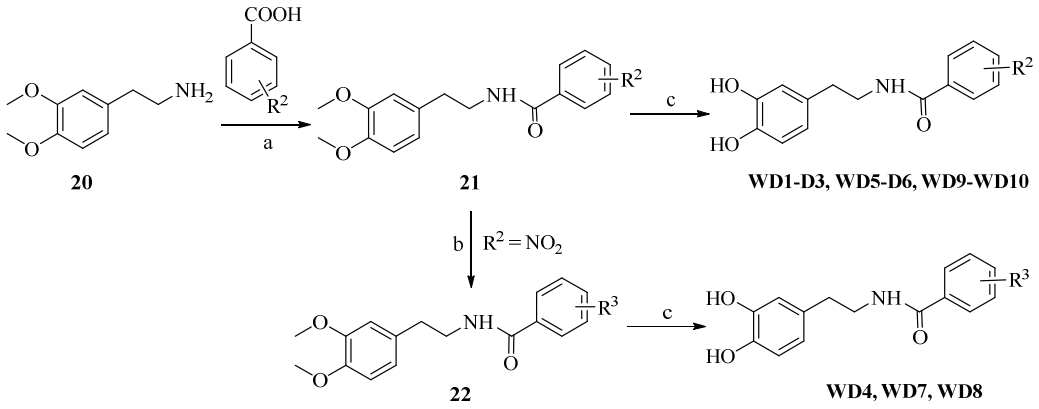

WD1 R^2 = 4- t-butyl
WD2 R^2 = 2-hydroxyl
WD3 R^2 = 4-bromo
WD4 R^3 = 3,5-diamino
WD5 R^2 = 3,4-dihydroxyl
WD6 R^2 = 3,4,5-trihydroxyl
WD7 R^3 = 4-amino
WD8 R^3 = 2-amino
WD9 R^2 = 4-methyl
WD10 R^2 = 4-trifluoromethyl

Research Highlights

> Novel nordihydroguaretic acid (NDGA) analogues were designed and synthesized. > They were evaluated as AcrB inhibitors against the *E. coli* BW25113. > Nine analogues were found to increase the efficacy of a panel of antibiotics. > Biochemical and docking studies were performed to determine AcrB inhibition. > They demonstrated moderate improvement in potency as compared to NDGA.

Declaration of Interest Statement

The authors declare that this study was carried out only with public funding. There is no funding or no agreement with commercial for profit firms.

The corresponding author on behalf of all authors: Shutao Ma